scientific reports

OPEN

# A mechanical and simplified model for RC elements subjected to combined shear and axial tension

A. Deifalla[1]✉ & F. M. Mukhtar[2,3]

**Very little is known about the shear behavior of elements, in particular those subjected to axial tension. The shear accompanied by tensile forces could cause premature failure of reinforced concrete, which is sudden with minimal warning. Therefore, understanding the shear behavior of reinforced concrete (RC) elements, including those subjected to axial tension, is an ultimate goal of the worldwide research community. In the current study, a new shear mechanical model for RC elements subjected to axial tension is developed, which makes physical sense and explains the behavior. The model is strain-based, inspired by the critical crack theory model (CSCT). In addition, the proposed model extended CSCT (ECSCT) quantifies the effect of axial tension forces on the shear strength in terms of reduction in the compression zone depth and increase in the longitudinal strain. Moreover, the nonlinear trend observed in the literature was implemented using nonlinear multi-variable regression. The ECSCT is validated and compared with available design methods with respect to an extensive database, including 180 elements tested under shear and tension from 18 different research investigations. The ECSCT provided an accurate and physically sound model yet safe to an acceptable extent. Last but not least, a simplified model for the purpose of design is proposed. The simplified model was chosen based on the mechanical model and calibrated using the extensive experimental database. The simplified model provided an accurate and simple model, yet safe to an acceptable extent.**

Shear failure of reinforced concrete (RC) elements is sudden and should be carefully considered, in particular, those without stirrups or with stirrups[1–21]. In addition, RC elements subjected to shear combined with axial tension are still a dilemma[22–26], which occurs in many situations. Many studies have been conducted to understand the effect of axial tension on the shear strength of RC. However, the physical significance of the tensile force on the shear design is not well defined yet. Shear behavior of RC elements is a complex problem that involves many mechanisms, as shown in Fig. 1[27]. Those mechanisms include but are not limited to: (1) direct shear through the compression zone, (2) friction along the sides of the diagonal shear cracks, (3) dowel action through longitudinal reinforcements crossing the diagonal cracks, (4) residual tensile stresses transferred across the diagonal, (5) the aggregate interlock across the diagonal crack. Suppose the beam is subjected to tensile axial forces, the crack width and the longitudinal strain increase. On the other hand, the compression zone depth, the residual tensile strength, and the aggregate interlock decrease. Recently, Deifalla[26] recommended using the observed behavior to improve and simplify the current physically sound-based models. The current study aims to develop and propose a mechanical model for RC elements under combined shear and tension. Inspired by the critical shear crack theory[28], a mechanical model named extended critical shear crack theory (ECSCT) was developed to include the effect of tensile forces. The strength of the experimental database was calculated using the proposed model and compared with existing design codes. In addition, a simplified model was proposed, which was found to be better for design purposes.

[1]Department of Structural Engineering and Construction Management, Future University in Egypt, New Cairo City 11835, Egypt. [2]Department of Civil and Environmental Engineering, King Fahd University of Petroleum & Minerals, Dhahran 31261, Saudi Arabia. [3]Interdisciplinary Research Center for Construction and Building Materials, King Fahd University of Petroleum & Minerals, Dhahran, Saudi Arabia. ✉email: ahmed.deifalla@fue.edu.eg

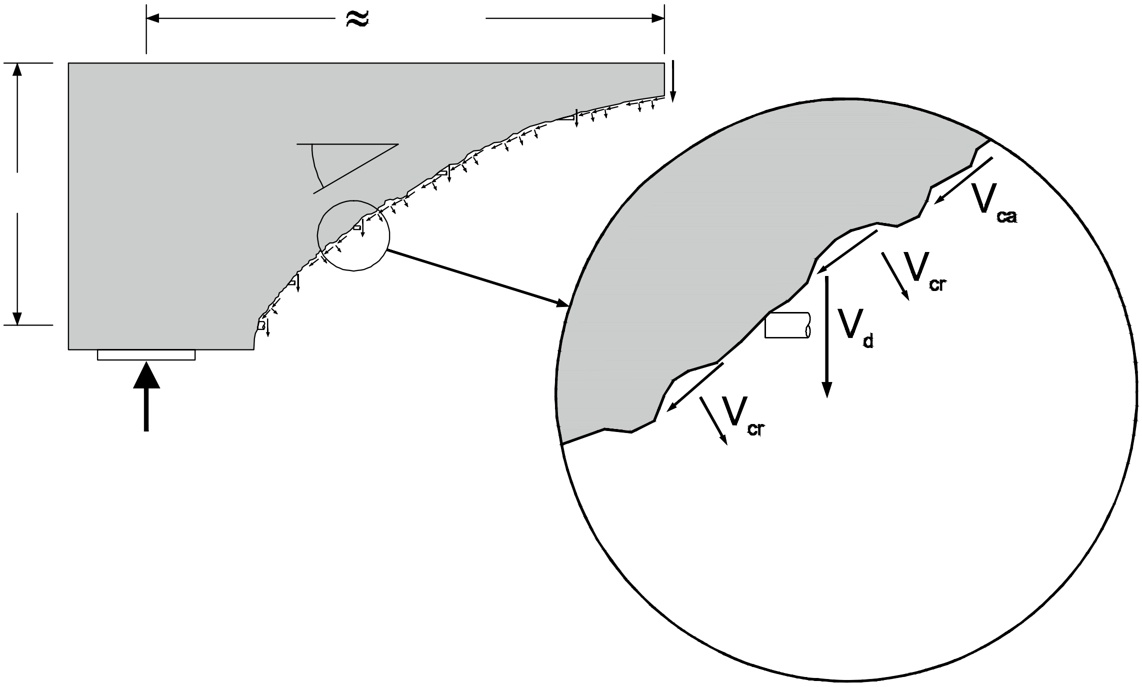


**Figure 1.** Shear failure mechanisms[27].

## Recent findings

For the last seven decades, several pioneering studies[26,29–33] have been conducted to investigate the shear strength of elements under axial tensile forces; a brief recount of the most recent findings is as follows.

- The significant variables that affect the shear strength are element dimensions, reinforcement configuration, loading configuration, and boundary conditions; thus, the conclusions of different studies were inconsistent with each other[31]. For example, the device used to apply the axial tension could cause accidental restraint at the ends of the tested element[33].
- The angle of inclination of shear cracking is significantly affected by the axial tension, which makes it steeper[33]. On the other hand, the shear strength of beams with well-detailed longitudinal reinforcements is not affected by axial tension. This is due to the aggregate interlock mechanism. In addition, the compression longitudinal steel reinforcements decrease the effect of axial tension forces on shear, if any[29].
- A nonlinear relationship between the axial everyday tensile stresses and the shear strength was found by several researchers[32]. This contradicts the long-standing linear relation implemented by both the ACI[34] and the EC2[35].
- Pham[31] observed a decrease in the compression zone depth with the increase in the axial tensile forces, as shown in Fig. 2.
- In general, design codes, including but not limited to the ACI and the EC2, are overly conservative, especially for cases of high tensile forces[26].
- An extensive experimental database of elements tested under shear and tension was gathered, combining the database complied by Deifalla[26] and Ehmann[30]. A total of 180 elements from 17 different research investigations. The data covered a wide range of all influential variables, as shown in Table 1 and Fig. 3[30–33,36–49]. The effective parameters included the axial tension, the size, the shear-span to depth ratio, the concrete strength, flexure reinforcement ratio, and the width to depth ratio were gathered.

## Model development

**Introduction.** This work is inspired by the Critical Shear Crack Theory (CSCT)[28], which was first introduced in the 1990s and later implemented in the swiss design code, MC, and the new draft of the Eurocode[26,50]. The shear strength ($v_u$) is calculated such that:

$$\frac{v_u}{\sqrt{f_c'}} = \mathrm{f}(\omega, \mathrm{d}_{dg}) \tag{1}$$

while ω is the crack width, $f_c'$ is the cylinder compressive strength and $d_{dg}$ is the maximum nominal aggregate size.

$$\omega \propto \varepsilon d \tag{2}$$

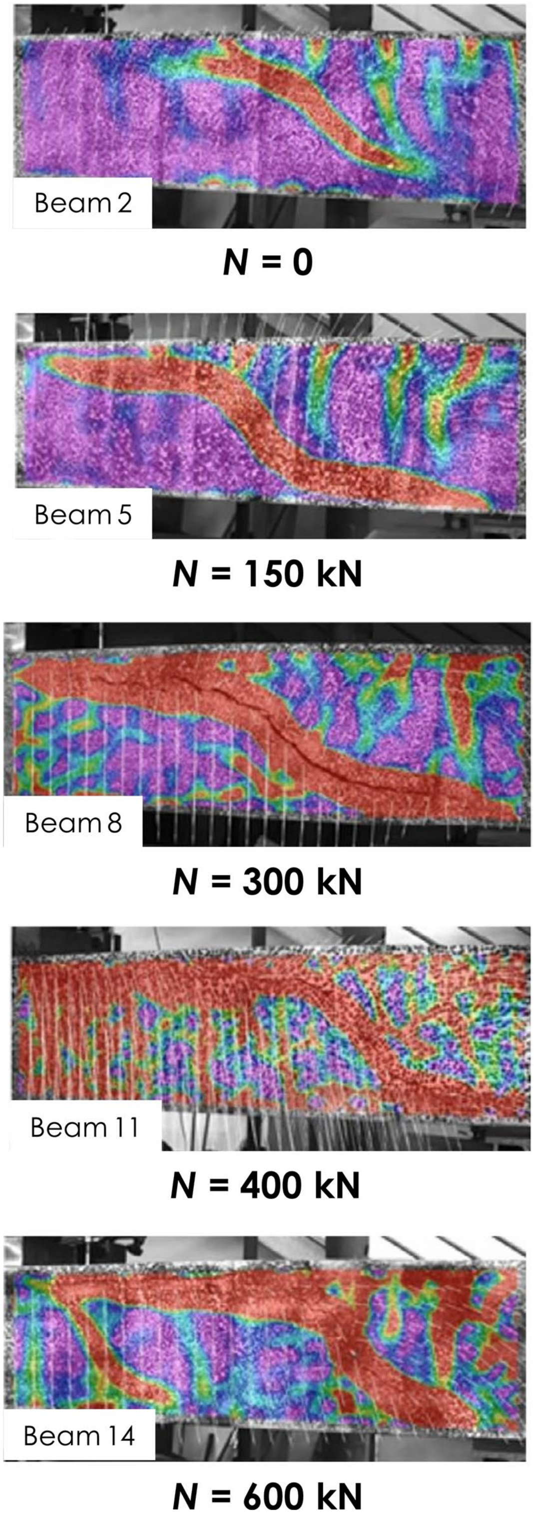


**Figure 2.** Experimentally observed behavior of RC beams under combined shear and tension[31].

where $d$ is the effective depth, and $\varepsilon$ is the longitudinal strain, which is taken at 60% of the effective depth from extreme compression fibers[28]. In addition, the following assumptions were implemented, which are similar to the work by Deifalla[24,25] for slabs under combined punching shear and tension: (1) Plane cross-sections before deformation remain plain after deformation,m while maintaining small deformation. (2) Concrete in compression is linear elastic behavior. (3) Concrete in tension is neglected. (4) Steel reinforcements reached yield. (5) The superposition principle applies to the longitudinal strains from flexure and tension. Figure 4a–c shows the

| References | Label | d (mm) | b (mm) | fc′ (MPa) | $\rho$ (–) | fy (MPa) | a/d (–) | N (kN) | V (kN) |
|---|---|---|---|---|---|---|---|---|---|
| [36] | 9 | 284 | 175 | 23 | 0.41% | 343.4 | 3.69 | 86 | 19.68 |
| | 10 | 284 | 175 | 23 | 0.41% | 343.4 | 3.69 | 68 | 24.13 |
| [37] | 4 | 254 | 152 | 46 | 1.03% | 399.9 | 3.00 | 29 | 44.48 |
| | 5 | 254 | 152 | 16 | 2.07% | 399.9 | 3.00 | 29 | 33.36 |
| | 11 | 254 | 152 | 15 | 3.10% | 399.9 | 3.00 | 61 | 42.26 |
| | 16 | 254 | 152 | 30 | 1.03% | 399.9 | 5.40 | 48 | 28.02 |
| | 19 | 254 | 152 | 19 | 2.07% | 399.9 | 5.40 | 29 | 40.03 |
| | 20 | 254 | 152 | 48 | 2.07% | 399.9 | 5.40 | 29 | 57.83 |
| | 21 | 254 | 152 | 51 | 2.07% | 399.9 | 5.40 | 61 | 56.93 |
| | 23 | 254 | 152 | 19 | 3.10% | 399.9 | 5.40 | 29 | 42.26 |
| | 25 | 254 | 152 | 28 | 3.10% | 399.9 | 5.40 | 48 | 51.15 |
| | 26 | 254 | 152 | 29 | 1.00% | 399.9 | 5.40 | 80 | 42.26 |
| | 29 | 254 | 152 | 53 | 3.10% | 399.9 | 5.40 | 29 | 66.72 |
| [38] | A1T | 381 | 178 | 28 | 3.78% | 517.3 | 2.50 | 144 | 122.55 |
| | C1T | 381 | 178 | 29 | 3.78% | 517.3 | 3.38 | 144 | 120.21 |
| | J1T | 381 | 178 | 29 | 3.78% | 517.3 | 2.50 | 144 | 87.00 |
| [39] | N3 | 272 | 152 | 33 | 1.46% | 427 | 2.80 | 120 | 42.00 |
| | N4 | 272 | 152 | 34 | 1.46% | 427 | 2.80 | 90 | 42.00 |
| | N5 | 272 | 152 | 32 | 1.46% | 427 | 2.80 | 60 | 48.00 |
| | N6 | 272 | 152 | 32 | 1.46% | 427 | 2.80 | 70 | 50.00 |
| | N7 | 272 | 152 | 35 | 1.46% | 427 | 2.80 | 130 | 45.00 |
| | N9 | 272 | 152 | 31 | 1.46% | 427 | 2.80 | 85 | 42.00 |
| | N11 | 272 | 152 | 33 | 0.97% | 427 | 2.80 | 75 | 37.00 |
| | N12 | 272 | 152 | 28 | 1.46% | 628 | 5.61 | 30 | 48.00 |
| | N13 | 272 | 152 | 31 | 1.46% | 628 | 5.61 | 40 | 50.00 |
| | N14 | 272 | 152 | 31 | 1.46% | 427 | 2.80 | 40 | 50.00 |
| | N15 | 272 | 152 | 32 | 1.46% | 427 | 2.80 | 20 | 50.00 |
| | N16 | 272 | 152 | 31 | 1.46% | 628 | 1.96 | 40 | 52.00 |
| | N18 | 272 | 152 | 31 | 1.46% | 427 | 2.80 | 60 | 45.00 |
| | N19 | 272 | 152 | 29 | 1.46% | 427 | 2.80 | 80 | 40.00 |
| | N20 | 272 | 152 | 46 | 1.46% | 427 | 2.80 | 60 | 42.00 |
| | N21 | 272 | 152 | 15 | 1.46% | 427 | 2.80 | 60 | 40.00 |
| | N22 | 272 | 152 | 32 | 1.46% | 427 | 1.96 | 60 | 85.00 |
| | N23 | 272 | 152 | 35 | 1.46% | 427 | 1.96 | 20 | 75.00 |
| | N24 | 272 | 152 | 22 | 1.46% | 427 | 2.80 | 60 | 37.00 |
| [40] | M5 | 250 | 760 | 21 | 0.4% | 602 | 4.00 | 295 | 137.30 |
| | M6 | 250 | 760 | 27 | 0.5% | 643 | 4.00 | 393 | 137.30 |
| [41] | T4 | 262 | 200 | 53 | 1.8% | 534 | 2.50 | 327 | 94.00 |
| | T5 | 262 | 200 | 53 | 1.8% | 534 | 2.50 | 439 | 81.90 |
| | T6 | 262 | 200 | 53 | 1.8% | 534 | 2.50 | 223 | 126.50 |
| [42] | PB4 | 890 | 70 | 16 | 1.1% | 423 | N/A | 72 | 72.30 |
| | PB6 | 890 | 70 | 17 | 1.1% | 425 | N/A | 72 | 71.60 |
| | PB7 | 890 | 70 | 20 | 1.1% | 425 | N/A | 102 | 53.60 |
| | PB8 | 890 | 70 | 20 | 1.1% | 425 | N/A | 148 | 49.20 |
| | PB10 | 890 | 70 | 24 | 1.1% | 425 | N/A | 148 | 34.90 |
| | PB16 | 890 | 70 | 42 | 1.1% | 502 | N/A | 181 | 90.30 |
| | PB14 | 890 | 70 | 42 | 2.0% | 489 | N/A | 288 | 95.90 |
| | PB17 | 890 | 70 | 25 | 2.0% | 502 | N/A | 449 | 76.00 |
| | PB19 | 890 | 70 | 20 | 2.0% | 402 | N/A | 80 | 79.70 |
| | PB20 | 890 | 70 | 22 | 2.0% | 411 | N/A | 177 | 88.50 |
| | PB28 | 890 | 70 | 23 | 2.0% | 424 | N/A | 191 | 95.30 |
| | PB21 | 890 | 70 | 22 | 2.0% | 426 | N/A | 274 | 88.50 |
| | PB22 | 890 | 70 | 18 | 2.0% | 402 | N/A | 392 | 64.20 |
| | PB29 | 890 | 70 | 42 | 2.0% | 433 | N/A | 186 | 92.80 |
| | PB30 | 890 | 70 | 40 | 2.0% | 496 | N/A | 277 | 92.20 |
| | PB31 | 890 | 70 | 43 | 2.0% | 496 | N/A | 422 | 71.60 |
| Continued | | | | | | | | | |

| References | Label | d (mm) | b (mm) | fc′ (MPa) | ρ (–) | fy (MPa) | a/d (–) | N (kN) | V (kN) |
|---|---|---|---|---|---|---|---|---|---|
| [43] | ZS2 | 164 | 600 | 40 | 4.0% | 500 | 3.05 | 1200 | 356.00 |
| [44] | P1 | 178 | 600 | 35 | 0.2% | 477 | 3.82 | 60 | 92.00 |
| | P2 | 178 | 600 | 35 | 0.2% | 477 | 3.82 | 60 | 92.00 |
| | P3 | 178 | 600 | 43 | 0.2% | 477 | 3.82 | 60 | 92.00 |
| | P4 | 178 | 600 | 43 | 0.6% | 506 | 3.82 | 60 | 92.00 |
| | P5 | 178 | 600 | 35 | 0.6% | 506 | 3.82 | 60 | 92.00 |
| [45] | ST9 | 278 | 290 | 46 | 1.95% | 536 | 3.60 | 280 | 69.90 |
| | ST10 | 278 | 290 | 46 | 1.95% | 536 | 3.60 | 525 | 65.60 |
| | ST11 | 278 | 290 | 46 | 1.95% | 536 | 3.60 | 776 | 65.60 |
| | ST12 | 278 | 290 | 46 | 1.95% | 536 | 3.60 | 1507 | 47.10 |
| | ST13 | 278 | 290 | 46 | 1.95% | 536 | 3.60 | 1050 | 65.60 |
| | ST25 | 278 | 290 | 59 | 1.00% | 484 | 3.60 | 165 | 82.00 |
| | ST26 | 278 | 290 | 59 | 1.00% | 484 | 3.60 | 191 | 58.90 |
| [46] | S1 | 204 | 80 | 37 | 0.87% | 356.5 | 2.00 | 30 | 32.75 |
| | S2 | 204 | 80 | 37 | 0.87% | 356.5 | 2.00 | 50 | 28.85 |
| | S3 | 204 | 80 | 37 | 0.87% | 356.5 | 2.00 | 60 | 27.95 |
| | S4 | 204 | 80 | 37 | 0.87% | 356.5 | 2.00 | 70 | 23.85 |
| | S5 | 204 | 80 | 37 | 0.87% | 356.5 | 2.50 | 30 | 27.00 |
| | S6 | 204 | 80 | 37 | 0.87% | 356.5 | 2.50 | 50 | 23.80 |
| | S7 | 204 | 80 | 37 | 0.87% | 356.5 | 2.50 | 60 | 23.35 |
| | S8 | 204 | 80 | 37 | 0.87% | 356.5 | 2.50 | 70 | 22.30 |
| | S10 | 204 | 100 | 37 | 1.26% | 356.5 | 2.00 | 20 | 30.03 |
| | S11 | 204 | 100 | 37 | 1.26% | 356.5 | 2.00 | 30 | 24.34 |
| | S12 | 204 | 100 | 37 | 1.26% | 356.5 | 2.00 | 40 | 23.00 |
| | S14 | 204 | 100 | 37 | 1.26% | 356.5 | 2.50 | 20 | 24.15 |
| | S15 | 204 | 100 | 37 | 1.26% | 356.5 | 2.50 | 30 | 19.42 |
| | S16 | 204 | 100 | 37 | 1.26% | 356.5 | 2.50 | 40 | 15.43 |
| Continued | | | | | | | | | |

| References | Label | d (mm) | b (mm) | fc′ (MPa) | ρ (–) | fy (MPa) | a/d (–) | N (kN) | V (kN) |
|---|---|---|---|---|---|---|---|---|---|
| 30 | A1 | 250 | 400 | 47 | 1.6% | 579 | 3.00 | 450 | 150.00 |
| | A2 | 250 | 400 | 47 | 1.6% | 579 | 3.00 | 340 | 146.60 |
| | A2′ | 250 | 400 | 47 | 1.6% | 579 | 5.00 | 340 | 122.90 |
| | A3 | 250 | 400 | 49 | 1.6% | 579 | 3.00 | 560 | 119.80 |
| | A3′ | 250 | 400 | 49 | 1.6% | 579 | 5.00 | 560 | 124.50 |
| | A4 | 250 | 400 | 49 | 2.5% | 559 | 3.00 | 340 | 162.50 |
| | A4′ | 250 | 400 | 49 | 2.5% | 559 | 5.00 | 340 | 134.10 |
| | A5 | 250 | 400 | 49 | 1.0% | 585 | 3.00 | 340 | 146.30 |
| | B2 | 250 | 400 | 46 | 2.0% | 558 | 3.00 | 200 | 122.50 |
| | B3 | 250 | 400 | 46 | 2.0% | 558 | 3.00 | 400 | 164.40 |
| | B3′ | 250 | 400 | 46 | 2.0% | 558 | 5.00 | 400 | 132.70 |
| | B4 | 250 | 400 | 46 | 2.0% | 558 | 3.00 | 600 | 109.80 |
| | B4′ | 250 | 400 | 46 | 2.0% | 558 | 5.00 | 600 | 125.20 |
| | B5 | 250 | 400 | 48 | 2.0% | 558 | 3.00 | 800 | 139.40 |
| | B5′ | 250 | 400 | 48 | 2.0% | 558 | 5.00 | 800 | 113.30 |
| | B6 | 250 | 400 | 46 | 1.0% | 572 | 3.00 | 200 | 137.30 |
| | B7 | 250 | 400 | 44 | 1.6% | 546 | 3.00 | 200 | 144.60 |
| | B7′ | 250 | 400 | 44 | 1.6% | 546 | 5.00 | 200 | 109.00 |
| | B8 | 250 | 400 | 45 | 2.5% | 570 | 3.00 | 200 | 150.20 |
| | B9 | 250 | 400 | 45 | 2.8% | 566 | 3.00 | 200 | 150.80 |
| | B9′ | 250 | 400 | 45 | 2.8% | 566 | 5.00 | 200 | 143.60 |
| | B10 | 250 | 400 | 48 | 1.0% | 572 | 3.00 | 600 | 94.10 |
| | B11 | 250 | 400 | 47 | 1.6% | 546 | 3.00 | 600 | 160.10 |
| | B11′ | 250 | 400 | 47 | 1.6% | 546 | 5.00 | 600 | 126.30 |
| | B12 | 250 | 400 | 47 | 2.5% | 570 | 3.00 | 600 | 174.00 |
| | B12′ | 250 | 400 | 47 | 2.5% | 570 | 5.00 | 600 | 140.70 |
| | C1 | 250 | 400 | 43 | 1.6% | 559 | 3.00 | 200 | 249.60 |
| | C1′ | 250 | 400 | 43 | 1.6% | 559 | 5.00 | 200 | 149.70 |
| | C2 | 250 | 400 | 43 | 1.6% | 559 | 3.00 | 600 | 136.10 |
| | C2′ | 250 | 400 | 43 | 1.6% | 559 | 5.00 | 600 | 153.20 |
| | C4 | 250 | 400 | 44 | 1.6% | 559 | 4.00 | 150 | 144.20 |
| | C4′ | 250 | 400 | 44 | 1.6% | 559 | 4.00 | 150 | 136.10 |
| | C5 | 250 | 400 | 44 | 1.6% | 559 | 4.00 | 340 | 138.50 |
| | C7 | 250 | 400 | 44 | 1.6% | 559 | 4.00 | 150 | 129.80 |
| | C7′ | 250 | 400 | 44 | 1.6% | 559 | 4.00 | 150 | 125.10 |
| | C8 | 250 | 400 | 45 | 1.6% | 559 | 4.00 | 340 | 127.60 |
| | C8′ | 250 | 400 | 45 | 1.6% | 559 | 4.00 | 340 | 116.70 |
| | C9 | 250 | 400 | 27 | 2.0% | 554 | 4.00 | 500 | 105.20 |
| | C10 | 250 | 400 | 52 | 2.0% | 554 | 3.00 | 500 | 146.00 |
| | C11 | 250 | 400 | 45 | 1.5% | 550 | 3.00 | 340 | 146.40 |
| | C12 | 250 | 400 | 45 | 1.5% | 550 | 3.00 | 600 | 151.20 |
| | C12′ | 250 | 400 | 45 | 1.5% | 550 | 5.00 | 600 | 143.00 |
| | C13 | 250 | 400 | 46 | 2.0% | 554 | 3.00 | 900 | 111.20 |
| | C13′ | 250 | 400 | 46 | 2.0% | 554 | 5.00 | 900 | 134.50 |
| Continued | | | | | | | | | |

| References | Label | d (mm) | b (mm) | fc′ (MPa) | ρ (–) | fy (MPa) | a/d (–) | N (kN) | V (kN) |
|---|---|---|---|---|---|---|---|---|---|
| 47 | ST-1 | 165 | 200 | 25 | 1.1% | 1027 | 2.25 | 427 | 39.50 |
| | ST-2 | 165 | 200 | 26 | 1.1% | 1027 | 2.25 | 97 | 43.50 |
| | ST-3 | 165 | 200 | 26 | 1.1% | 1027 | 2.25 | 200 | 45.40 |
| | ST-6 | 165 | 200 | 27 | 1.1% | 1027 | 2.25 | 300 | 43.00 |
| | ST-7 | 165 | 200 | 27 | 1.1% | 1027 | 2.25 | 401 | 40.80 |
| | ST-8 | 165 | 200 | 27 | 1.1% | 1027 | 2.25 | 499 | 39.80 |
| | ST-9 | 165 | 200 | 27 | 1.1% | 1027 | 2.25 | 299 | 45.40 |
| | ST-10 | 165 | 200 | 28 | 1.1% | 1027 | 2.25 | 401 | 36.90 |
| | ST-12 | 165 | 200 | 28 | 1.1% | 1027 | 2.25 | 200 | 44.00 |
| | ST-13 | 165 | 200 | 29 | 1.1% | 1027 | 2.25 | 100 | 33.90 |
| | ST-14 | 165 | 200 | 29 | 1.1% | 1027 | 2.75 | 201 | 40.70 |
| | ST-15 | 165 | 200 | 29 | 1.1% | 1027 | 2.75 | 301 | 44.60 |
| | ST-17 | 165 | 200 | 30 | 1.1% | 1027 | 2.75 | 100 | 39.90 |
| | ST-18 | 165 | 200 | 30 | 1.1% | 1027 | 2.75 | 200 | 32.80 |
| | ST-19 | 165 | 200 | 30 | 1.1% | 1027 | 2.75 | 300 | 32.00 |
| | ST-20 | 165 | 200 | 30 | 1.1% | 1027 | 2.75 | 500 | 30.20 |
| | ST-22 | 165 | 200 | 30 | 1.1% | 1027 | 2.75 | 501 | 37.50 |
| | ST-23 | 165 | 200 | 30 | 1.1% | 1027 | 2.25 | 602 | 34.50 |
| | ST-24 | 165 | 200 | 30 | 1.1% | 1027 | 2.25 | 600 | 35.20 |
| 48 | V8-1 | 164 | 140 | 36 | 1.00% | 495 | 1.97 | 30 | 57.37 |
| | V8-2 | 164 | 140 | 82 | 1.00% | 495 | 1.97 | 51 | 75.73 |
| | V8-3 | 164 | 140 | 34 | 1.00% | 495 | 1.97 | 50 | 45.13 |
| | V8-4 | 164 | 140 | 34 | 1.00% | 495 | 1.97 | 102 | 50.91 |
| | V9-1 | 164 | 140 | 31 | 1.51% | 487 | 1.97 | 27 | 68.94 |
| | V9-2 | 164 | 140 | 74 | 1.51% | 487 | 1.97 | 47 | 71.95 |
| | V9-3 | 164 | 140 | 36 | 1.51% | 487 | 1.97 | 60 | 52.83 |
| | V9-4 | 164 | 140 | 74 | 1.51% | 495 | 1.97 | 69 | 109.90 |
| | V9-5 | 164 | 140 | 33 | 1.51% | 495 | 1.97 | 109 | 58.09 |
| | V9-6 | 164 | 140 | 82 | 1.51% | 487 | 1.97 | 154 | 52.63 |
| 33 | ST1 | 267 | 4000 | 34 | 1.15% | 500 | 4.59 | 600 | 711.00 |
| | ST2 | 267 | 4000 | 35 | 1.15% | 500 | 4.59 | 780 | 742.00 |
| | ST3 | 267 | 4000 | 34 | 1.15% | 500 | 4.59 | 1200 | 539.00 |
| | ST4 | 267 | 4000 | 34 | 1.15% | 500 | 4.59 | 1440 | 555.00 |
| 49 | SC8 | 267 | 4000 | 35 | 1.15% | 500 | 4.59 | 1200 | 801.00 |
| | SC9 | 267 | 4000 | 33 | 1.15% | 500 | 4.59 | 1800 | 792.00 |
| 32 | N1-1 | 255 | 300 | 38 | 1.00% | 957 | 4.53 | 259 | 73.00 |
| | N1-2 | 255 | 300 | 39 | 1.00% | 957 | 4.53 | 258 | 70.00 |
| | N2-1 | 255 | 300 | 38 | 1.00% | 957 | 4.53 | 195 | 102.00 |
| | N2-2 | 255 | 300 | 39 | 1.00% | 957 | 4.53 | 195 | 55.00 |
| | N3-1 | 255 | 300 | 38 | 1.00% | 957 | 4.53 | 317 | 68.00 |
| | N3-2 | 255 | 300 | 39 | 1.00% | 957 | 4.53 | 317 | 116.00 |
| 31 | 4 | 280 | 200 | 33 | 1.65% | 550 | 3.57 | 147 | 68.00 |
| | 5 | 280 | 200 | 33 | 1.65% | 550 | 3.57 | 147 | 51.00 |
| | 6 | 280 | 200 | 35 | 1.65% | 550 | 3.57 | 148 | 59.00 |
| | 7 | 280 | 200 | 33 | 1.65% | 550 | 3.57 | 298 | 60.00 |
| | 8 | 280 | 200 | 33 | 1.65% | 550 | 3.57 | 297 | 48.00 |
| | 9 | 280 | 200 | 35 | 1.65% | 550 | 3.57 | 297 | 56.00 |
| | 10 | 280 | 200 | 34 | 1.65% | 550 | 3.57 | 397 | 43.00 |
| | 11 | 280 | 200 | 34 | 1.65% | 550 | 3.57 | 397 | 61.00 |
| | 12 | 280 | 200 | 35 | 1.65% | 550 | 3.57 | 397 | 62.00 |
| | 13 | 280 | 200 | 34 | 1.65% | 550 | 3.57 | 596 | 63.00 |
| | 14 | 280 | 200 | 34 | 1.65% | 550 | 3.57 | 596 | 60.00 |
| | 15 | 280 | 200 | 35 | 1.65% | 550 | 3.57 | 594 | 73.00 |
| Average | | 296 | 370 | 37 | 1.5% | 563 | 3.35 | 292 | 100.05 |
| Minimum | | 164 | 70 | 15 | 0.2% | 343 | 1.96 | 20 | 15.43 |
| Maximum | | 890 | 4000 | 82 | 4.0% | 1027 | 5.61 | 1800 | 801 |

**Table 1.** Experimental database.

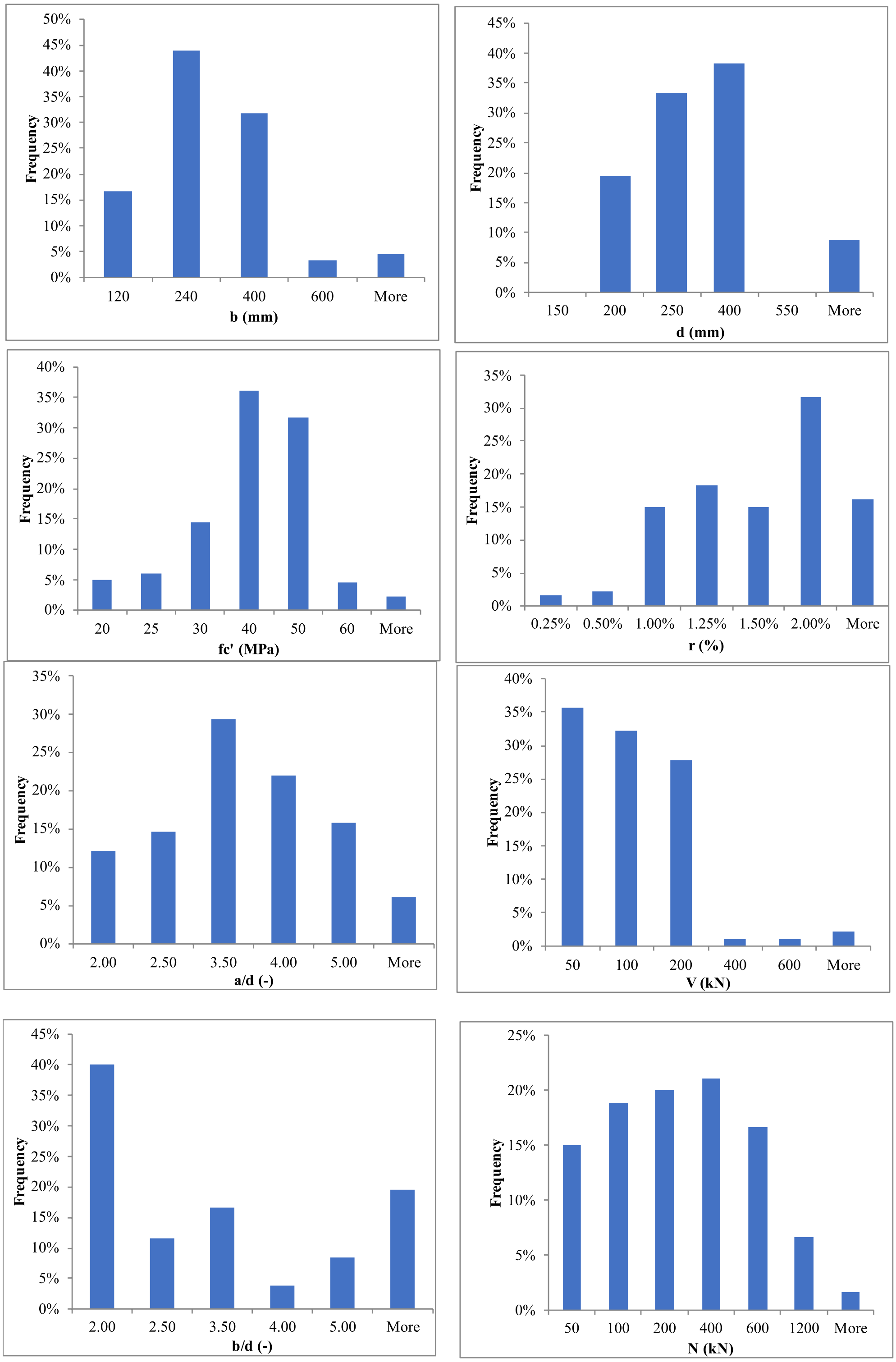


**Figure 3.** The profile of data base.

distribution diagrams for a) flexure only, b) tensile forces only, and c) both, respectively; thus, the tensile strain at 60% of the effective depth from extreme compression fibers (ε), which is calculated such that:

$$\varepsilon = \frac{1}{bd\boldsymbol{\rho}E_s}\left[\frac{M}{d\left(1-\boldsymbol{\rho}\cdot\frac{E_s}{E_c}\left(\sqrt{1+\frac{2E_c}{\boldsymbol{\rho}\cdot E_s}}-1\right)/3\right)}+\frac{N}{2}\right]\left(\frac{0.6d-c}{d-c}\right) \tag{3}$$

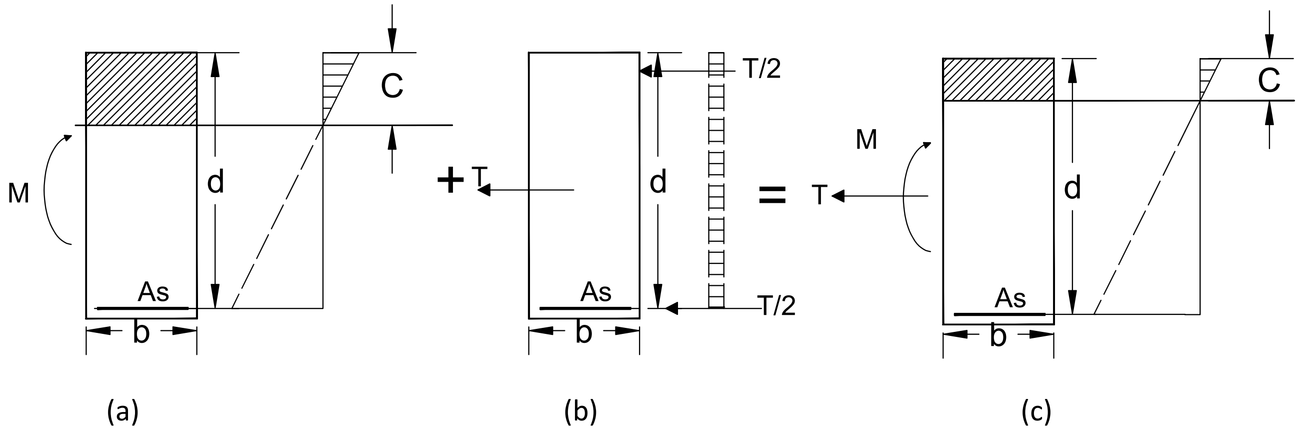


**Figure 4.** Strain diagram for (**a**) flexure only, (**b**) tension only, and (**c**) flexure and tension.

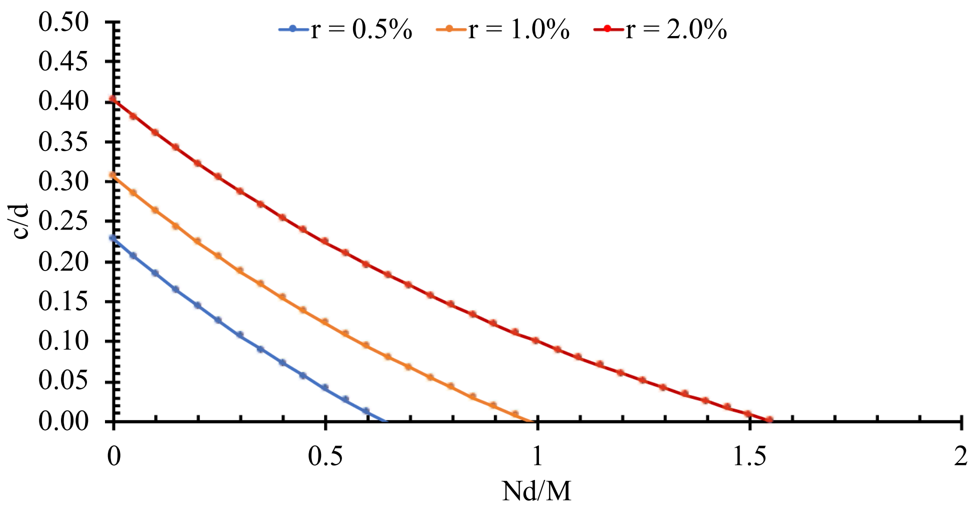


**Figure 5.** The effect of tension forces on the compression zone depth of elements with different reinforcement ratios ($fc' = 30$ MPa and $M/Vd = 4$).

where $b$ is the element width, $\boldsymbol{\rho}$ is the flexure reinforcement ratio, $N$ is the axial force ( positive is tension and negative is compression), $M$ is the bending moment at the critical section for shear, $E_s$ is the steel reinforcements young's modulus (210,000 MPa), $E_c$ is the concrete young's modulus ($10{,}000\sqrt[3]{f_c'}$), $c$ is the compression zone depth, which is calculated such that:

$$\frac{c}{d} = \boldsymbol{\rho} \cdot \frac{E_s}{E_c}\left(\sqrt{1 + \frac{2E_c}{\boldsymbol{\rho} \cdot E_s}} - 1\right) - \frac{Nd/M}{\left[\frac{2}{\left(1-\boldsymbol{\rho}\cdot\frac{E_s}{E_c}\left(\sqrt{1+\frac{2E_c}{\boldsymbol{\rho}\cdot E_s}}-1\right)/3\right)} + \frac{Td}{M}\right]} \tag{4}$$

Figure 5 shows the variation of the compression zone depth (Eq. 4) versus the tensile stress for different flexure reinforcement ratios. Figure 5 was based on $f_c'$ value of 30 MPa and $M/Vd$ value of 4, where V is the shear force at the critical section for shear. It is clear that the model captured the reduction in the compression zone depth observed by Pham[31].

**Proposed failure criteria for combined shear and tension.** Based on data shown in Table 1 and Fig. 3 as well as the failure criteria of the CSCT, the following form was proposed:

$$\frac{v_u}{\sqrt{f_c'}} = \frac{\alpha_1}{1 + \alpha_2 \frac{\varepsilon d}{d_{dg}}} \tag{5}$$

Using nonlinear multi-variable regression, thus, the shear stress is calculated such that:

| Parameter | Estimate | Standard error | t-Statistic | p-value |
|---|---|---|---|---|
| $\alpha_1$ | 0.27 | 0.019 | 13.7 | 7.79E−30 |
| $\alpha_2$ | 22 | 8.47 | 2.56 | 0.011 |

**Table 2.** Parameter table for ECSCT.

| Parameter | Estimate | Standard error | t-statistic | p-value | Lower 95% | Upper 95% |
|---|---|---|---|---|---|---|
| $c_1$ | 17.22 | 0.530 | 5.37 | 2.53E−07 | 6.047 | 49.05 |
| $c_2$ | 0.010 | 0.042 | 0.24 | 0.81 | −0.074 | 0.094 |
| $c_3$ | 0.077 | 0.017 | 4.41 | 1.81E−05 | 0.042 | 0.111 |
| $c_4$ | 0.34 | 0.042 | 8.00 | 1.65E−13 | 0.258 | 0.427 |
| $c_5$ | 0.40 | 0.063 | 6.29 | 2.39E−09 | 0.273 | 0.523 |
| $c_6$ | −0.70 | 0.064 | −11 | 1.56E−21 | −0.83 | −0.576 |
| $c_7$ | −0.39 | 0.054 | −7.1 | 2.31E−11 | −0.495 | −0.281 |

**Table 3.** Parameter table for simplified model.

$$\frac{v_u}{\sqrt{f_c'}} = \frac{0.27}{1 + 22\frac{\varepsilon d}{d_{dg}}} \tag{6}$$

for shear and tension. Where $v_u = \frac{V}{bd}$, $d_{dg} = d_{g0} + d_g$ (the value of the reference aggregate size $d_{g0} = 16$ mm is used), and $d_g$ is the maximum nominal aggregate size. Table 2 shows the parameter table for the coefficient $\alpha_1$ and $\alpha_2$.

## Simplified model

### Model development.

In this section, a simplified model is developed. Based on the proposed mechanical model presented in Eqs. (3), (4) and (6), the following parameters are identified to be effective in the shear strength of elements subjected to axial tensile forces: (1) $M/Nd$, (2) $N/(bd\boldsymbol{\rho}f_y)$, (3) $M/Vd$ or $a/d$, (4) $d$, (5) $f_c'$, and (6) $\rho$. Thus, nonlinear multi-variable regression was performed using the following power form:

$$v_u = \boldsymbol{c}_1\left(N/(bd\boldsymbol{\rho}f_y)\right)^{\boldsymbol{c}_2}(M/Nd)^{\boldsymbol{c}_3}\boldsymbol{\rho}^{\boldsymbol{c}_4}f_c'^{\boldsymbol{c}_5}(M/Vd)^{\boldsymbol{c}_6}\boldsymbol{d}^{\boldsymbol{c}_7} \tag{7}$$

Power form was implemented in several investigations (Ali et al., 2021; Deifalla et al., 2021; Deifalla, 2020b; 2020c; 2021b; 2021c). Table 3 shows the parameter table, including the probability of each parameter. It is worth noting that the power coefficient of the variable $N/(bd\boldsymbol{\rho}f_y)$ failed the hypotheses test, and it was found to be insignificant. Therefore, it is proposed that shear strength is calculated such that:

$$v_u = 17.22(\mathrm{M/Nd})^{0.077}\boldsymbol{\rho}^{0.34}f_c'^{0.4}(M/Vd)^{-0.7}d^{-0.39} \tag{8}$$

## Models validation

For simplicity, two design codes were selected for comparison: the ACI and the EC2. However, it is worth noting that there is other design model that are more accurate with various levels of approximation, for example fib model code[50]. For simplicity, the model code was not selected as it requires a detailed calculation compared to the ACI and EC2. The strength calculated using the ECSCT and the simplified model were assessed against those calculated using the selected design codes with respect to the experimentally measured strength.

Several types of figures were implemented to compare the performance of the proposed models with the selected design codes, which were implemented in several investigations[12,51–54]. Firstly: a scatter plot between the measured and calculated strength was plotted for all models, which was assessed using the ideal 45-degree line and the inverse of the slope of the best-fitted line. While the strength in terms of stress is taken as the ratio between the shear force and the concrete cross area. Secondly: a histogram figure for the distribution of the ratio between measured and calculated strength (SR), which is assessed based on the distribution and being far from the ideal ratio of unity and lower coefficient of variation. The unity value for SR indicates the closeness of the calculated value to the measured one (i.e., the model accuracy). At the same time, the coefficient of variation of the SR distribution indicates the consistency of the model. In addition, the lower 95% of the SR indicates the safety of the model. It is the minimum SR value obtained using the model with a 95% confidence level. Therefore, the higher value of the lower 95% limit above the safety factor of design codes (approximately 0.85), the safer the model is. The confidence interval is calculated assuming a standard normal distribution. In addition, a significant level value of 0.05 represents the 95% confidence level. Thus, the lower 95% confidence limit is calculated using the following expression:

$$\text{Lower } 95\% = \text{Average} - 1.96\left(\frac{\text{Standard deviation}}{\sqrt{\text{number of samples}}}\right) \tag{8}$$

Thirdly: a scatter plot for the SR against various effective parameters is plotted, which is assessed using the inclination of the best-fitted line and the correlation coefficient ($r$). The closer the slope to zero is the more negligible effect of the variable on the accuracy and safety of the model. The $r$ is the degree of association, which is such that:

$$r = \left|\frac{\sum_{i=1}^{n}(x_i - \overline{x})(y_i - \overline{y})}{\sqrt{\sum_{i=1}^{n}(x_i - \overline{x})^2}\sqrt{\sum_{i=1}^{n}(y_i - \overline{y})^2}}\right| \tag{9}$$

where, $\overline{x}$ and $\overline{y}$ are average values of variables $x_i$ and $y_i$, respectively, and n is the number of tested specimens. The correlation coefficient is measured on a scale that varies from $\pm 1$ to 0. For example, $\pm 1$, $\pm 0.70$, $\pm 0.50$, $\pm 0.30$, and zero indicate exact, strong, moderate, weak, and no dependence, respectively. Thus, if the r value is less than $\pm 0.30$ shows that the model captured the effect of such parameter, while a coefficient ranged between $\pm 0.50$ and $\pm 0.30$ indicates a need for refinements in the modeling of this parameter. It is worth noting that the correlation coefficient is not directly related to the data scattering. Because the data scattering is dependent on the overall effect of the considered parameters in the specific model, while the correlation coefficient is indicative of the relation between the accuracy and a specific parameter. It is an indication not conclusive depending on the value as mentioned before.

**Overall.** Figure 6 shows the calculated shear strength versus the measured ones for the ECSCT, the simplified model, the ACI, and the EC2. While the strength is calculated in terms of stress taken as the ratio between the shear force and the concrete cross area. In addition, the line represents the actual performance and the linear fitted line for the model performance. Moreover, the inverse of the best-fitted line slope ($\chi$) is indicated in the plots. The closer this value to unity is, the better accuracy and less divergence. The $\chi$ value for the ECSCT, the simplified model, the ACI, and the EC2 is 0.99, 0.88, 0.50, and 0.65. Thus, the strength calculated using the ECSCT and the simplified model is significantly less scattered than using the ACI and EC2.

Moreover, Fig. 6 shows the histogram of the SR values calculated using the ECSCT, the simplified model, the ACI, and the EC2. The SR is calculated using the simplified model, and the ECSCT is normally distributed around the ratio of unity compared to that using the ACI and the EC2. Last but not least, Table 4 shows the average, coefficient of variation, and lower 95% limit for SR calculated using the ECSCT, the simplified model, the ACI, and the EC2 for each study. It is clear that the performance of the ECSCT and the simplified model is more accurate and consistent than that of the ACI and EC2. However, it is safe with a lower 95% value of 0.96, higher than 0.85 targeted by most design codes. The simplified model and ECSCT SR values have a narrow range compared to that calculated using the ACI and the EC2, as shown in Table 4.

**Effect of axial tension ($N$).** The effect of the axial tension was examined using several parameters, namely $N/(bdf_{ct})$, $N/(\boldsymbol{\rho bdf_y})$, $N/V$ and $M/Nd$. The SR is plotted against the $N/(bdf_{ct})$, $N/(\boldsymbol{\rho bdf_y})$, $N/V$ and $M/Nd$ as shown in Figs. 7, 8, 9 and 10, respectively, where $f_{ct}$ is the tensile concrete strength taken as $0.65\sqrt[2]{f_c'}$, $f_y$ is the yield stress of the steel reinforcements. From Figs. 7, 8, 9 and 10, the safety of the strength calculated using the ECSCT and the simplified model is more consistent with the axial tension's effect than the ACI and EC2. The correlation coefficient (r) was calculated as 0.51–0.67, 0.54–0.73, 0.02–0.14, and 0.04–0.25 for the ACI, the EC2, the ECSCT, the simplified model, respectively. In addition, the slope of the best fit line for the SR calculated using the ACI, the EC2, is much higher than that calculated using the ECSCT, the simplified model. Thus, it is clear that SR calculated using the ECSCT and the simplified model are weakly correlated to the axial tension, while the ACI and EC2 are highly correlated· The variation of the tensile axial force does not affect the ECSCT and the simplified model compared to the ACI and the EC2 with respect to the experimental database.

**Effect of shear span to depth ratio ($a/d$).** The SR is plotted against the specimen size in the shear span to depth ratio (a/d), as shown in Fig. 11. From Fig. 11, the safety of the strength calculated using the ECSCT and the simplified model is more consistent with the effect of the $a/d$ compared with the ACI and EC2. However, the safety for the ECSCT is higher for non-slender elements with $a/d$ value less than 3. This is because the original CSCT model was not developed for non-slender. In addition, the correlation coefficient (r) was calculated as 0.46, 0.49, 0.40, and 0.09 for the ACI, the EC2, the ECSCT, the simplified model, respectively. Thus, it is clear that SR calculated using the simplified model is weakly correlated to the $a/d$, while the ECSCT, the ACI, and EC2 are highly correlated to the $a/d$.

Moreover, the slope of the best fit line for the SR calculated using the ACI, the EC2, the ECSCT, and the simplified model is 0.46, 0.56, 0.10, and 0.02, respectively. The slope for the SR calculated using the ECSCT and simplified model is significantly lower than that calculated using the ACI and the EC2. The simplified model showed quite an improvement with respect to the effect of the arch mechanism in terms of the shear span to depth ratio (a/d).

**Effect of specimen size ($d$).** Plots of the SR versus the specimen size in terms of effective depth ($d$) are shown in Fig. 12. From Fig. 12, the safety of the strength calculated using the ECSCT and the simplified model is more consistent with the effect of the $d$ compared with the ACI and EC2. In addition, the correlation coef-

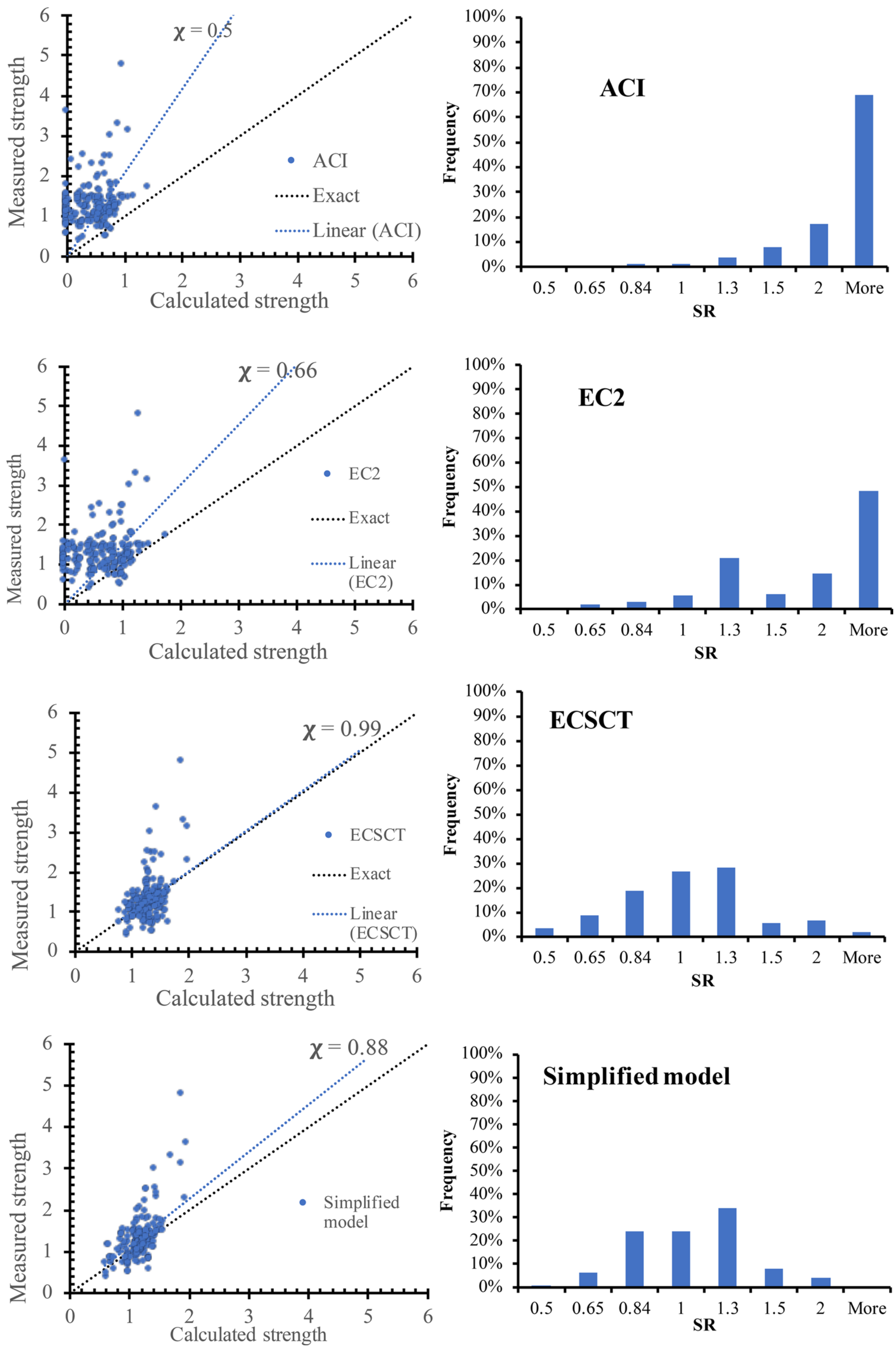


**Figure 6.** Measured Strength versus calculate strength using various methods.

ficient (r) was calculated as 0.26, 0.32, 0.04, and 0.25 for the ACI, the EC2, the ECSCT, and the simplified model, respectively. Thus, it is clear that SR calculated using the simplified model, the ECSCT is weakly correlated to the *d*. Moreover, the slope of the best fit line for the SR calculated using the ACI, the EC2, the ECSCT, and the simplified model is 2300E-6, 2900E-6, 70E-6, and 1E-6, respectively. Thus, the slope for the SR calculated using the ECSCT and simplified model is significantly lower than that calculated using the ACI and the EC2. Therefore, the ECSCT model and the simplified model account for the effect of size in terms of *d* much better than the ACI and the EC2.

**Effect of flexural reinforcement ratio (*ρ*).** The SR is plotted versus the size in terms of the flexure reinforcement ratio (*ρ*), as shown in Fig. 13. From Fig. 13, the safety of the strength calculated using the ECSCT and

| Refs. | Measure | Number | ACI-19 | EC2 | ECSCT | Simplified model |
|---|---|---|---|---|---|---|
| 36 | Mean | 2 | 1.80 | 0.95 | 0.48 | 0.74 |
| | Coefficient of variation | | 2% | 6% | 14% | 12% |
| 37 | Mean | 11 | 1.49 | 1.03 | 0.93 | 1.04 |
| | Coefficient of variation | | 22% | 17% | 16% | 20% |
| 38 | Mean | 3 | 2.11 | 1.40 | 1.25 | 0.95 |
| | Coefficient of variation | | 19% | 19% | 19% | 24% |
| 39 | Mean | 19 | 1.86 | 1.23 | 0.92 | 0.87 |
| | Coefficient of variation | | 23% | 21% | 24% | 22% |
| 40 | Mean | 2 | 3.00 | 1.58 | 0.85 | 1.19 |
| | Coefficient of variation | | 10% | 7% | 13% | 12% |
| 41 | Mean | 3 | 5.00 | 5.00 | 1.27 | 1.04 |
| | Coefficient of variation | | 0% | 0% | 21% | 18% |
| 42 | Mean | 16 | 5.00 | 4.62 | 1.16 | 1.23 |
| | Coefficient of variation | | 0% | 13% | 21% | 21% |
| 43 | Mean | 1 | 5.00 | 5.00 | 2.50 | 1.71 |
| | Coefficient of variation | | N/A | N/A | N/A | N/A |
| 44 | Mean | 5 | 2.84 | 1.53 | 0.73 | 1.02 |
| | Coefficient of variation | | 23% | 20% | 15% | 19% |
| 45 | Mean | 14 | 3.17 | 1.89 | 1.06 | 0.90 |
| | Coefficient of variation | | 48% | 43% | 28% | 27% |
| 46 | Mean | 7 | 3.25 | 2.75 | 0.56 | 0.64 |
| | Coefficient of variation | | 59% | 77% | 13% | 14% |
| 30 | Mean | 44 | 3.16 | 2.23 | 0.95 | 1.02 |
| | Coefficient of variation | | 43% | 50% | 18% | 18% |
| 47 | Mean | 19 | 4.73 | 4.46 | 1.11 | 0.93 |
| | Coefficient of variation | | 33% | 27% | 14% | 11% |
| 48 | Mean | 10 | 4.19 | 3.00 | 1.81 | 1.25 |
| | Coefficient of variation | | 18% | 27% | 22% | 17% |
| 33 | Mean | 4 | 0.83 | 0.59 | 0.44 | 0.62 |
| | Coefficient of variation | | 10% | 11% | 16% | 12% |
| 49 | Mean | 2 | 1.16 | 0.81 | 0.58 | 0.80 |
| | Coefficient of variation | | 11% | 16% | 3% | 3% |
| 32 | Mean | 6 | 2.80 | 1.70 | 0.88 | 1.15 |
| | Coefficient of variation | | 44% | 38% | 34% | 27% |
| 31 | Mean | 12 | 4.24 | 3.22 | 0.88 | 0.93 |
| | Coefficient of variation | | 32% | 53% | 18% | 14% |
| Overall | Mean | 180 | 3.3 | 2.5 | 1.01 | 0.99 |
| | Coefficient of variation | | 46% | 62% | 35% | 24% |
| | Minimum | | 0.73 | 0.5 | 0.37 | 0.50 |
| | Maximum | | 5 | 5 | 2.58 | 1.71 |
| | Lower 95.0% | | 3.07 | 2.3 | 0.96 | 0.96 |

**Table 4.** Statistical measures for the SR for shear with axial tension.

the simplified model is more consistent with the effect of the $\boldsymbol{\rho}$ compared with the ACI and EC2. In addition, the correlation coefficient (r) was calculated as 0.08, 0.00, 0.18, and 0.06 for the ACI, the EC2, the ECSCT, and the simplified model, respectively. Thus, it is clear that SR calculated using the ACI, the EC2, the ECSCT, and the simplified model is weakly correlated to the $\boldsymbol{\rho}$. Moreover, the slope of the best fit line for the SR calculated using

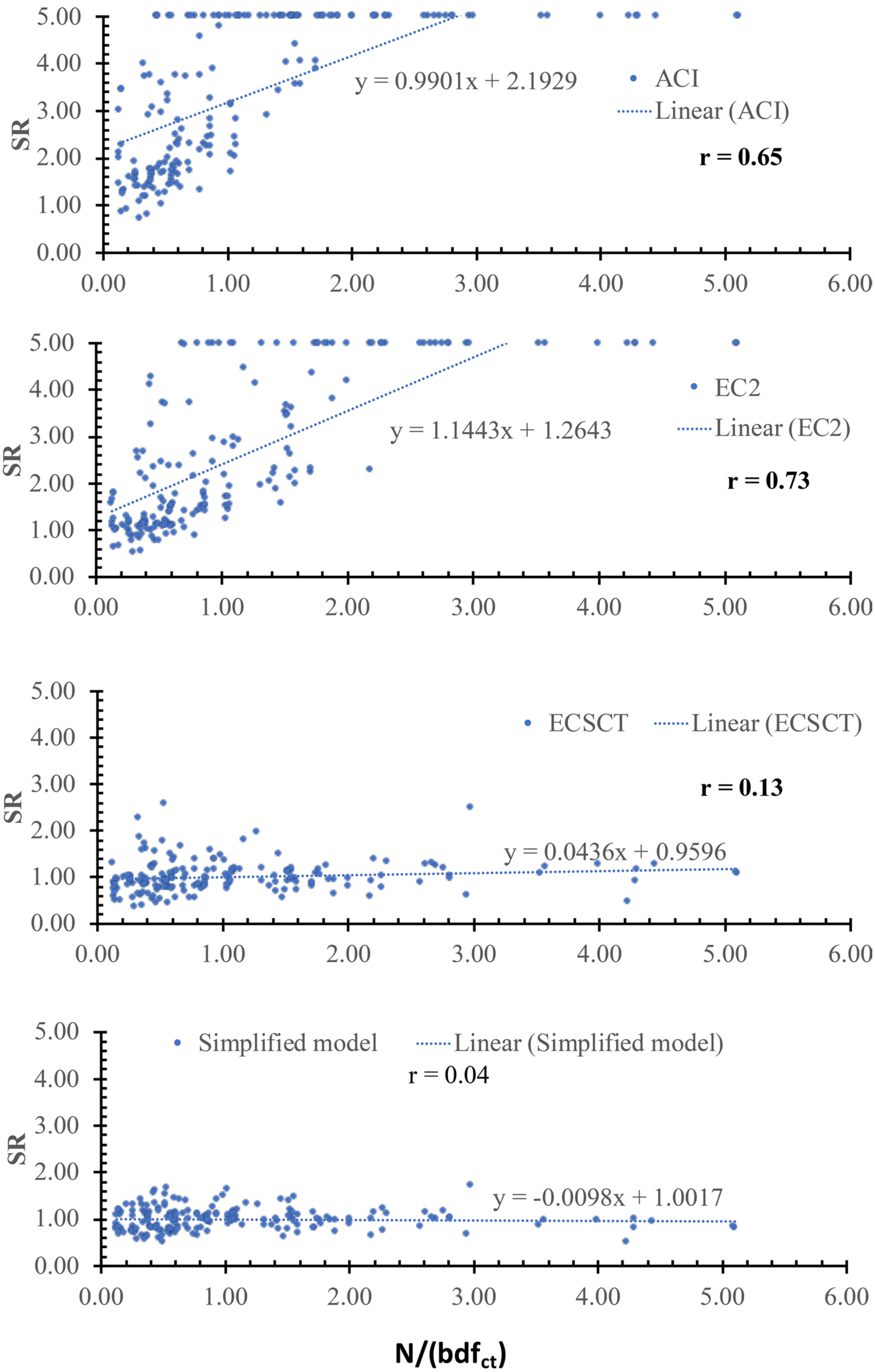


**Figure 7.** SR using various methods versus the $N/(bdf_{ct})$.

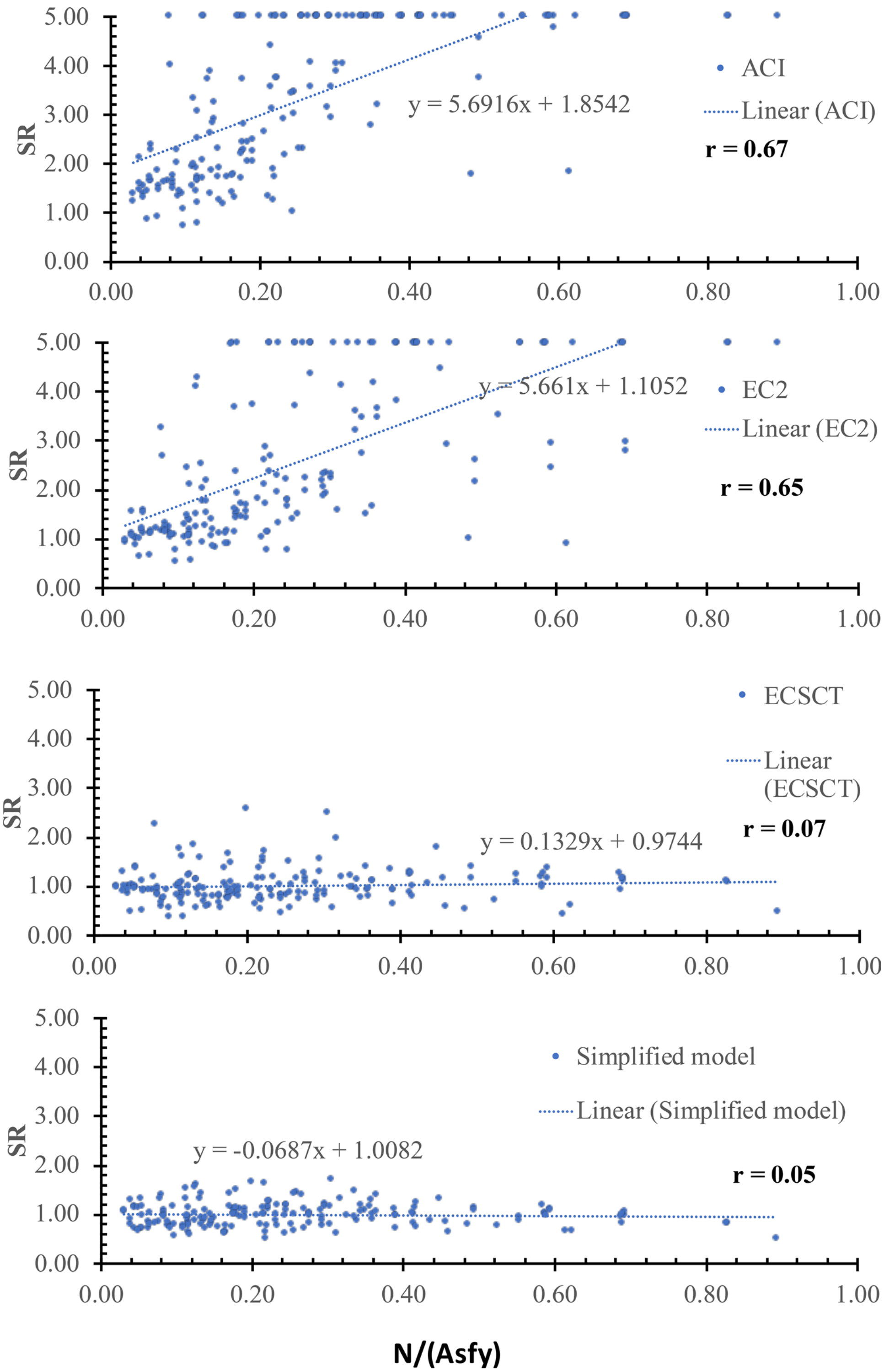


**Figure 8.** SR using various methods versus the $N/(\rho bdf_y)$.

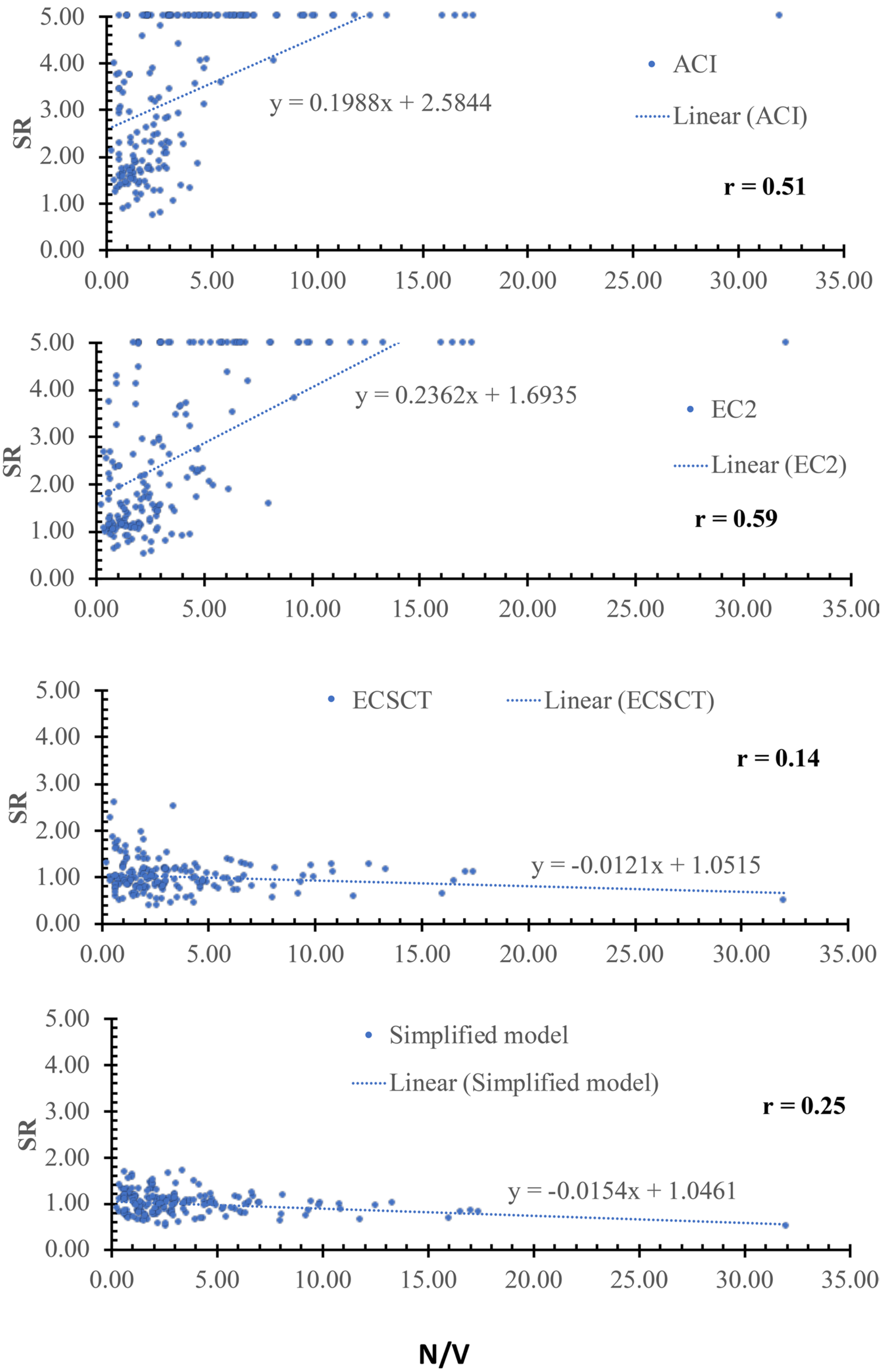


**Figure 9.** SR using various methods versus the *N*/*V*.

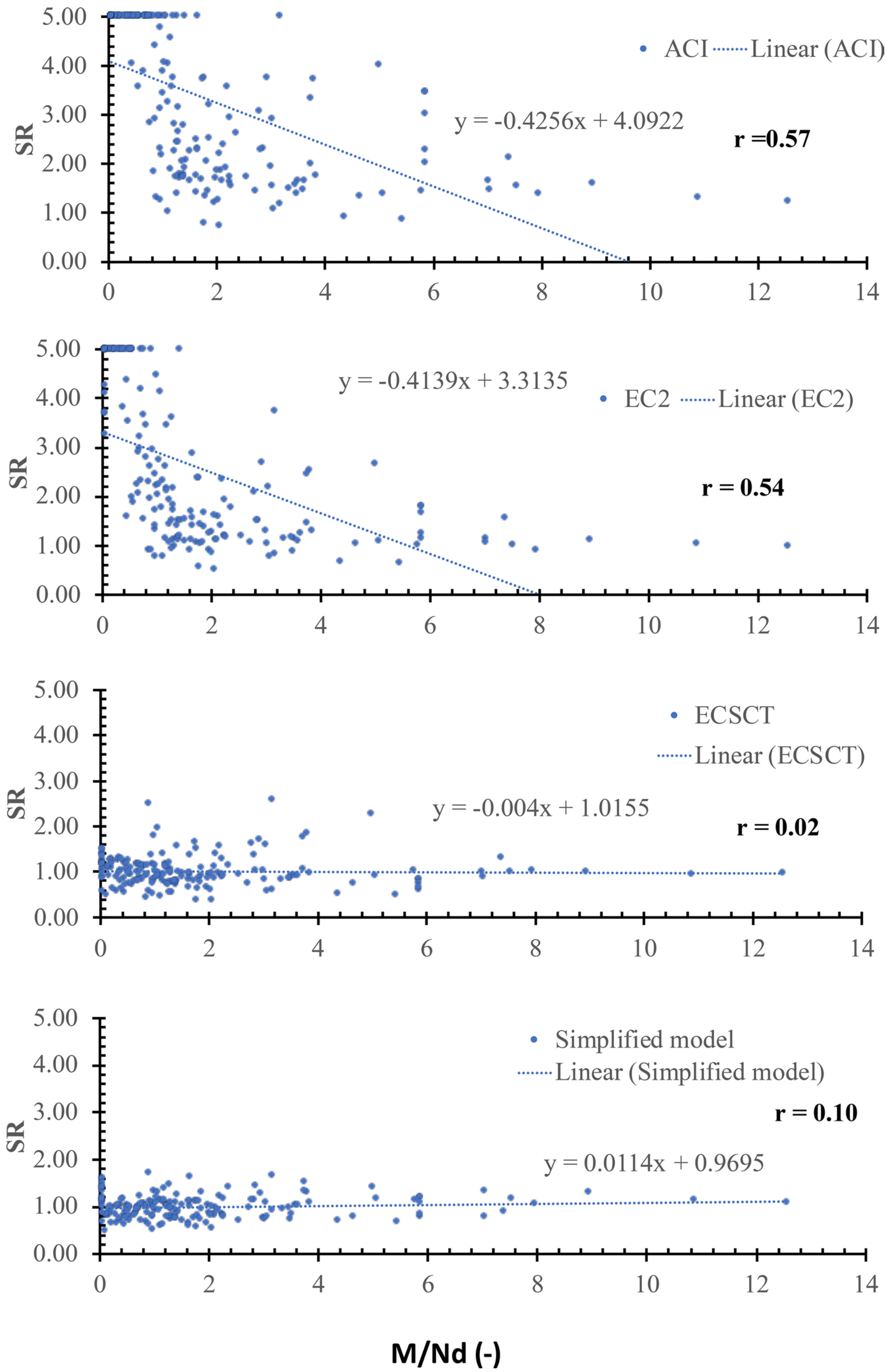


**Figure 10.** SR using various methods versus the *M*/*Nd*.

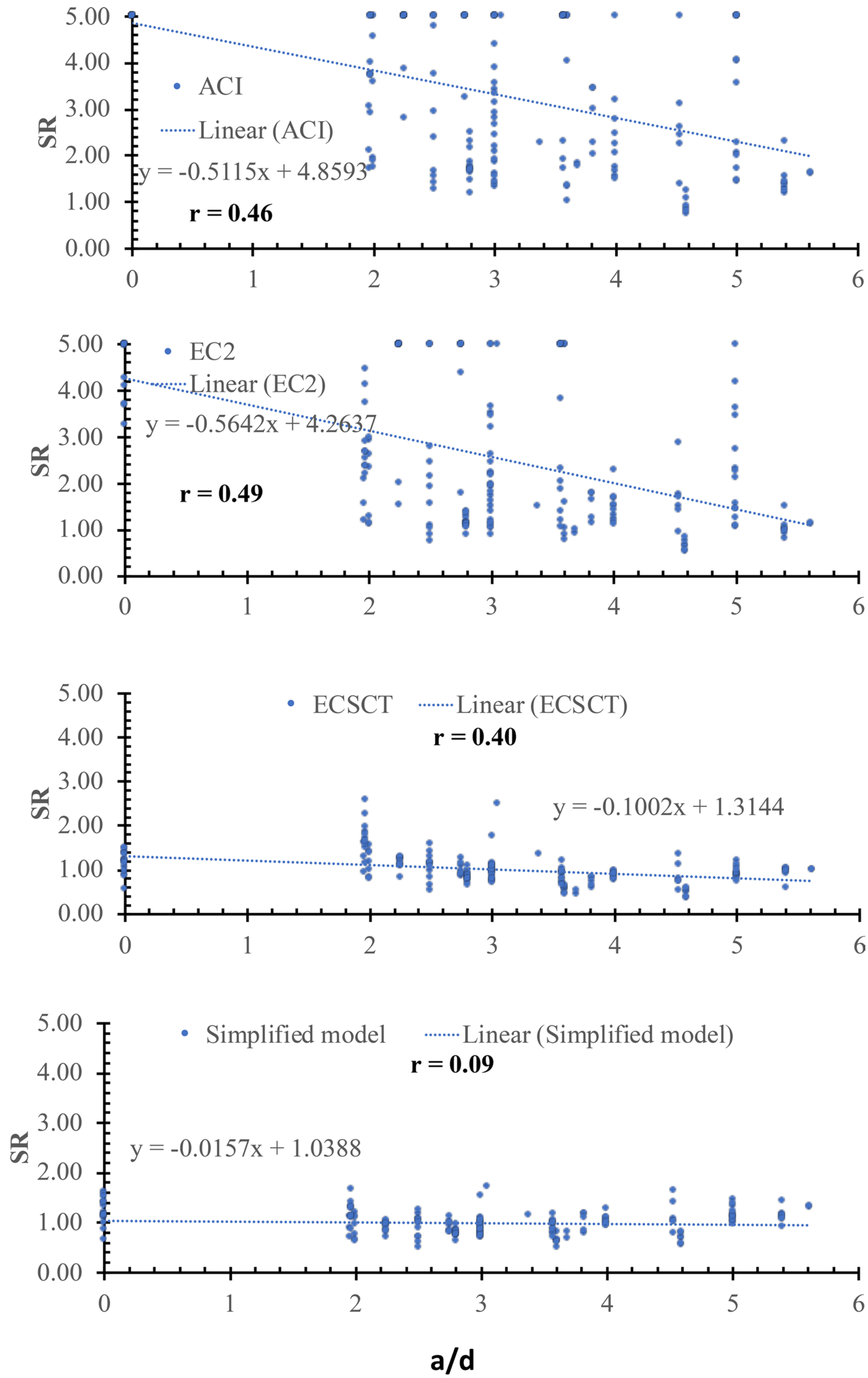


**Figure 11.** SR using various methods versus the *d*.

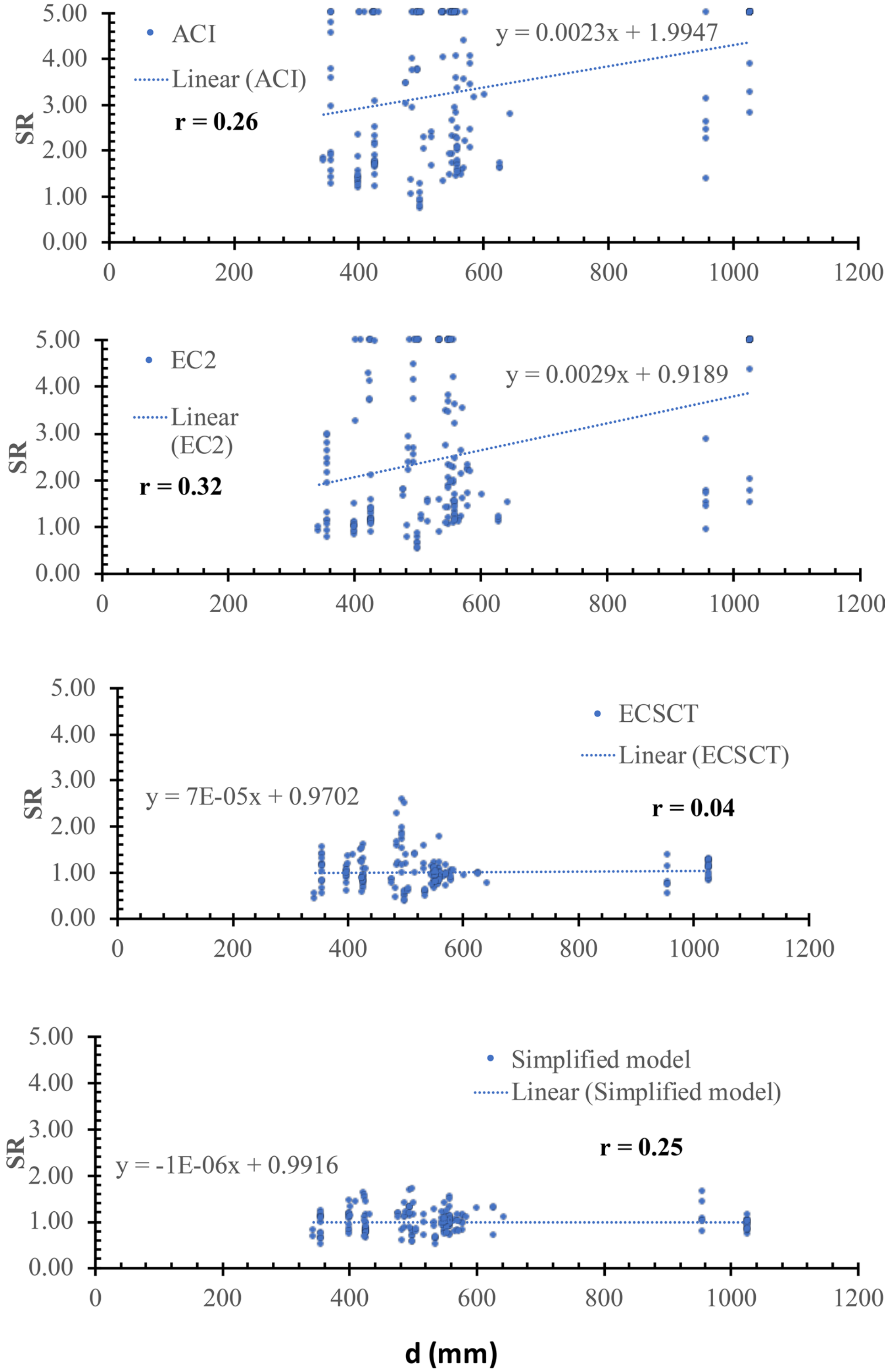


**Figure 12.** SR using various methods versus the *a*/*d*.

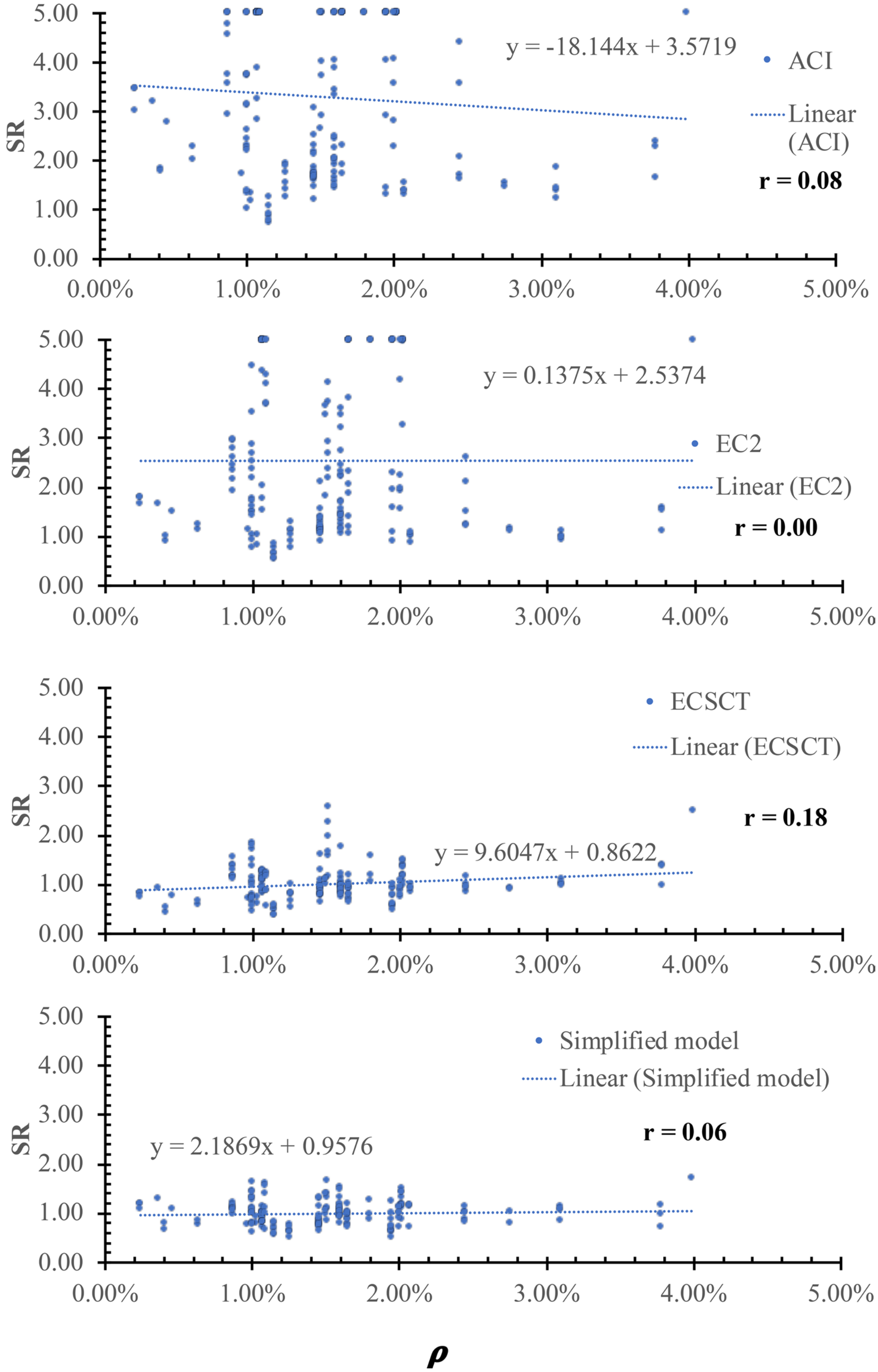


**Figure 13.** SR using various methods versus the $\rho$.

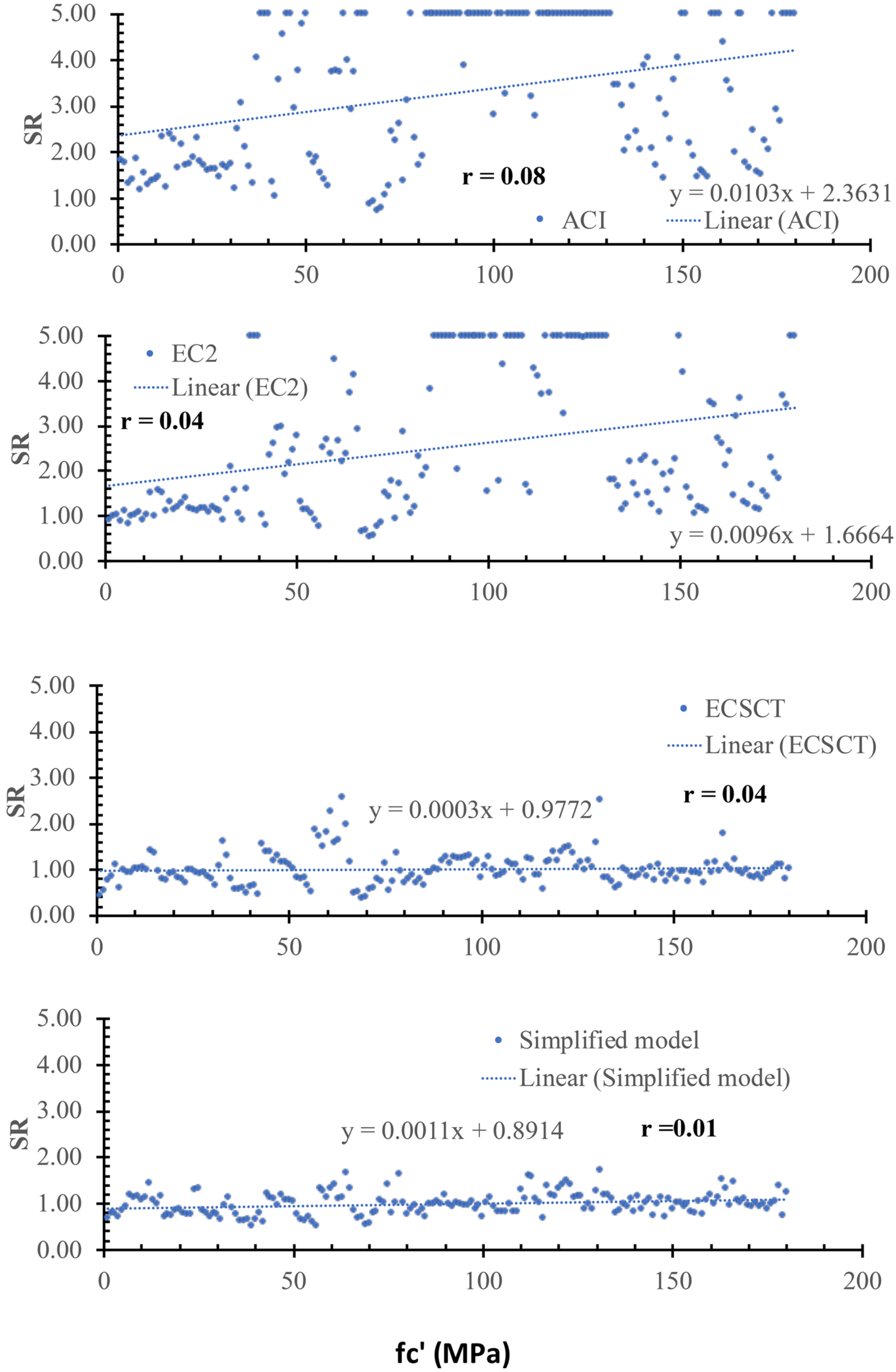


**Figure 14.** SR using various methods versus the fc′.

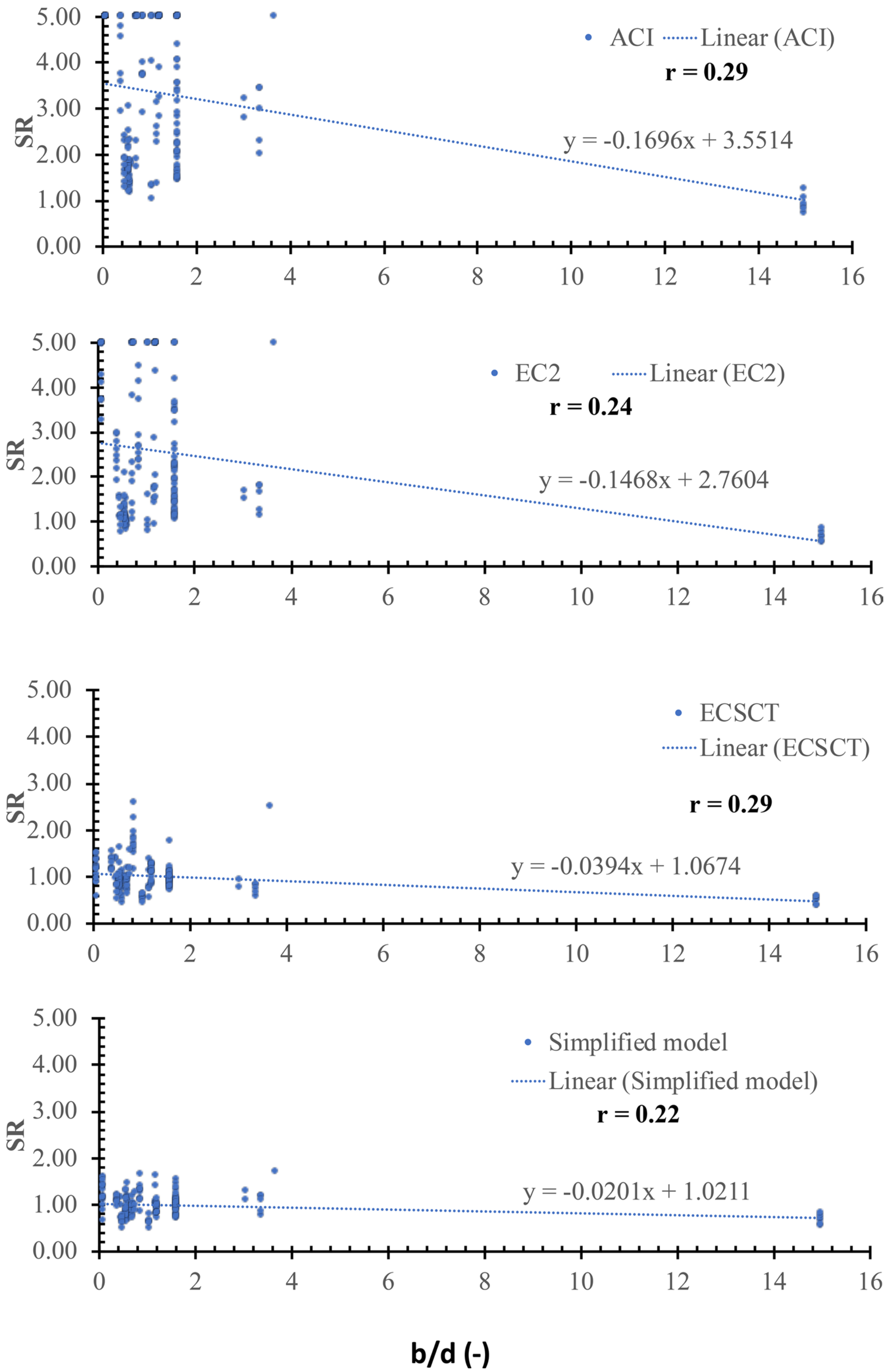


**Figure 15.** SR using various methods versus the b/d.

the ACI, the EC2, the ECSCT, and the simplified model is 18.4, 0.137, 9.6, and 2.2, respectively. Thus, the slope for the SR calculated using all models is similar. Therefore, it is clear that all models account for the dowel action mechanism in terms of the flexure reinforcement ratio.

**Effect of concrete compressive strength (*fc*′).** The SR is plotted versus the size in terms of the concrete compressive strength (*fc*′), as shown in Fig. 14. From Fig. 14, the safety of the strength calculated using the ECSCT and the simplified model is more consistent with the fc′ effect compared with the ACI and EC2.

In addition, the correlation coefficient (r) was calculated as 0.08, 0.04, 0.04, and 0.01 for the ACI, the EC2, the ECSCT, and the simplified model, respectively. Thus, it is clear that SR calculated using the ACI, the EC2, the ECSCT, and the simplified model is weakly correlated to the $fc'$. Moreover, the slope of the best fit line for the SR calculated using the ACI, the EC2, the ECSCT, and the simplified model is 103E-4, 96E-4, 3E-4, and 11E-4, respectively. Thus, the slope for the SR calculated using the ECSCT and simplified model is significantly lower than that calculated using the ACI and the EC2. Therefore, it is clear that the ECSCT and the simplified model are more consistent and accurate with respect to the direct shear mechanism and the residual tensile stresses in terms of the concrete strength ($fc'$).

**Effect of width to depth ratio ($b/d$).** The SR is plotted versus the size in terms of the width to depth ratio ($\mathbf{b}/\mathbf{d}$), as shown in Fig. 15. From Fig. 15, the safety of the strength calculated using the ECSCT and the simplified model is more consistent with the effect of the $\boldsymbol{b}/\boldsymbol{d}$ compared with the ACI and EC2. In addition, the correlation coefficient (r) was calculated as 0.29, 0.24, 0.29, and 0.22 for the ACI, the EC2, the ECSCT, and the simplified model, respectively. Thus, it is clear that SR calculated using the ACI, the EC2, the ECSCT, and the simplified model is moderately correlated to the $\boldsymbol{b}/\boldsymbol{d}$. Moreover, the slope of the best fit line for the SR calculated using the ACI, the EC2, the ECSCT, and the simplified model is 17E-2, 15E-2, 4E-2, and 2E-2, respectively. The slope for the SR calculated using the ACI and the EC2 is significantly higher than that calculated using the ECSCT and simplified model. Therefore, it is clear that the ECSCT and the simplified model are more consistent with respect to the aspect ratio.

## Conclusions

A physically sound mechanical model capable of accurately reproducing the actual behavior of reinforced concrete members under combined shear and tension is proposed. In addition, the model is accurate and simple for design. The effect of axial tensile forces on the compression zone depth and longitudinal strain and, ultimately, on the shear strength is accounted for. The proposed model is based on the principles of mechanics and its applicability to reinforced concrete elements under shear combined with tension. In addition, a simplified model is proposed for the purpose of design. The two proposed models were found to be more accurate, consistent, and reasonably safe compared to selected design codes. Moreover, the effect of basic parameters on the safety of the proposed models and the selected design codes was assessed. For all basic variables, including (1) the axial tension; (2) the shear span to depth ratio; (3) the flexure reinforcement ratio; (4) the concrete compressive strength; and (5) the width to dept ratio, the following conclusions were reached.

- The correlation relation with the safety factor calculated using the American and European design code was very strong, while that for the proposed models was very weak. Thus, the proposed models captured the effect of all basic variables much better than the selected design models.
- The slope of the best fit line for the safety factor calculated using the proposed models is very small compared to that using the selected design codes. Thus, the proposed models are more consistent with the basic variables than existing design codes.

## Data availability

All data generated or analysed during this study are included in this published article.

Received: 11 February 2022; Accepted: 26 April 2022
Published online: 12 May 2022

## References

1. Hu Biao, Wu. & Fei, Y. Quantification of shear cracking in reinforced concrete beams. *Eng. Struct.* **147**(2017), 666–678 (2017).
2. Biao, H. & Yu-Fei, W. Effect of shear span-to-depth ratio on shear strength components of RC beams. *Eng. Struct.* **168**(2018), 770–783 (2018).
3. Yu-Fei, W. & Biao, H. Shear strength components in reinforced concrete members. *J. Struct. Eng.* **143**(9), 04017092–04017101. https://doi.org/10.1061/(ASCE)ST.1943-541X.0001832 (2017).
4. Deifalla, A. & Ghobarah, A. Full torsional behavior of RC beams wrapped with FRP: Analytical model. *ACSE Compos. Construct.* **14**(3), 289–300 (2010).
5. Deifalla, A. & Ghobarah, A. Strengthening RC T-beams subjected to combined torsion and shear using FRP fabrics—Experimental study. *ASCE Compos. Construct.* **14**(3), 301–311 (2010).
6. Deifalla, A. & Ghobarah, A. Behavior and analysis of inverted T-shaped RC beams under shear and torsion. *Eng. Struct. Elsevier* **62**, 776–786 (2014).
7. Deifalla, A., Hamed, M., Saleh, A. & Ali, T. Exploring GFRP bars as reinforcement for rectangular and L-shaped beams subjected to significant torsion: An experimental study. *Eng. Struct. Elsevier* **59**, 776–786 (2014).
8. Deifalla, A., Khali, M. S. & Abdelrahman, A. Simplified model for the torsional strength of concrete beams with GFRP stirrups. *Compos. Construct. ASCE*. https://doi.org/10.1061/(ASCE)CC.1943-5614.0000498,04014032 (2015).
9. Deifalla, A., Awad, A., Seleem, H. & AbdElrahman, A. Investigating the behavior of lightweight foamed concrete T-beams under torsion, shear, and flexure. *Eng. Struct.* **219**(2020), 110741. https://doi.org/10.1016/j.engstruct.2020.110741 (2020).
10. Deifalla, A., Awad, A., Seleem, H. & AbdElrahman, A. Experimental and numerical investigation of the behavior of LWFC L-girders under combined torsion. *Structures.* **26**(2020), 362–377. https://doi.org/10.1016/j.istruc.2020.03.070 (2020).
11. Deifalla, A. Strength and ductility of lightweight reinforced concrete slabs under punching shear. *Structures* **27**, 2329–2345. https://doi.org/10.1016/j.istruc.2020.08.002 (2020).
12. Deifalla, A. Design of lightweight concrete slabs under two-way shear without shear reinforcements: A comparative study and a new model. *Eng. Struct. Elsevier* **222**(2020), 111076. https://doi.org/10.1016/j.engstruct.2020.111076 (2020).

13. Deifalla, A. Torsion design of lightweight concrete beams without or with fibers: A comparative study and a refined cracking torque formula. *Structures* **28**(2020), 786–802. https://doi.org/10.1016/j.istruc.2020.09.004 (2020).
14. El-Meligy, O., El-Nemr, A. M. & Deifalla, A. Re-evaluating the modified shear provision of CAN/CSA S806-12 for concrete beams reinforced with FRP stirrups. *AEI*. https://doi.org/10.1061/9780784480502.027 (2017).
15. Hassan, M. M. & Deifalla, A. Evaluating the new CAN/CSA-S806-12 torsion provisions for concrete beams with FRP reinforcements. *Mater. Struct.* https://doi.org/10.1617/s11527-015-0680-9 (2015).
16. Deifalla, A., Awad, A. & El-Garhy, M. Effectiveness of externally bonded CFRP strips for strengthening flanged beams under torsion: An experimental study. *Eng. Struct. Elsevier* **56**, 2065–2075 (2013).
17. Bara, H.C. (1971). Investigation on the effect of axial loads on the shear strength of reinforced concrete beams [PhD thesis]. Faculty of Engineering, Imperial College of Science and Technology, London.
18. Deifalla, A. F., Mousa, E., Yehia, D. & Abdelrahman, A. Exploring the effect of in-plane tensile forces on the two-way shear strength: Review, comparative study and future works. *Future Eng. J.* **2**(1), 5 (2021).
19. Ebid, A. & Deifalla, A. Prediction of shear strength of FRP reinforced beams with and without stirrups using (GP) technique. *Ain Shams Eng. J. Elsevier.* https://doi.org/10.1016/j.asej.2021.02.006 (2021).
20. Saleh, A., Fathy, A., Deifalla, A. & Nasser, M. Performance of steel fiber reinforced concrete corbels. *Int. Res. J. Innovat. Eng. Technol. IRJIET* **3**(2), 22–27 (2019).
21. Ali, A., Hamady, M., Chalioris, C.E., Deifalla, A. Evaluation of the shear design equations of FRP-reinforced concrete beams without shear reinforcement. *Eng. Struct. Elsevier*. **235** (2021).
22. Belletti, B., Damoni, C., Cervenka, V. & Hendriks, M. A. N. Catenary action effects on the structural robustness assessment of RC slab strips subjected to shear and tensile forces. *Struct. Concr.* **17**(6), 1003–1016 (2016).
23. Deifalla, A. Punching shear strength and deformation for FRP-reinforced concrete slabs without shear reinforcements. *Case Stud. Construct. Mater.* **16**, e00925. https://doi.org/10.1016/j.cscm.2022.e00925 (2022).
24. Deifalla, A. A mechanical model for concrete slabs subjected to combined punching shear and in-plane tensile forces. *Eng. Struct. Elsevier* **231**(2021), 111787. https://doi.org/10.1016/j.engstruct.2020.111787 (2021).
25. Deifalla, A. A comparative study and a simplified formula for punching shear design of concrete slabs with or without membrane tensile forces. *Structures* **33**, 1936–1953. https://doi.org/10.1016/j.istruc.2021.05.070 (2021).
26. Deifalla, A. Assessment of one-way shear design of RC elements subjected to axial tension. *Case Stud. Construct. Mater.* https://doi.org/10.1016/j.cscm.2021.e00620 (2021).
27. ASCE-ACI Committee 445 (1999). Report on recent shear. Joint ACI-ASCE Committee 445.
28. Muttoni, A. Punching shear strength of reinforced concrete slabs without shear reinforcement. *ACI Struct. J.* **105**(4), 440–450. https://doi.org/10.14359/19858 (2008).
29. Sayani, F.H.N. (1968). Influence of axial tension on the shear strength of reinforced concrete beams. M. Phil. Thesis, Imperial College of Science and Technology, University of London, 1968, 118.
30. Ehmann, J. (2003). Querkrafttragfahigkeit zugbeanspruchtwe Stahlbetonplatten in Verbundbrucken. Thesis submitted to Stuttgart Universty, Germany.
31. Pham, D. T., Fouré, B., Pinoteau, N., Abouri, S. & Mège, R. Influence of axial tension on the shear strength of RC beams without stirrups. *Struct. Concrete.* https://doi.org/10.1002/suco.202000077 (2020).
32. Adam, V., Claßen, M., Hegger, J. (2020). Tests on shear behavior with concurrent normal tensile action. Versuche zum Querkraft-trag-verhalten bei gleichzeitiger Zugnormalkraft. Beton und Stahlbeton bau. https://doi.org/10.1002/best.202000003.
33. Bui, T. T. *et al.* Influence of uniaxial tension and compression on shear strength of concrete slabs without shear reinforcement under concentrated loads. *Constr. Build. Mater.* **146**(2017), 86–101. https://doi.org/10.1016/j.conbuildmat.2017.04.068 (2017).
34. ACI-318 (2019), Committee 318. Building Code Requirements for Structural Concrete (ACI 318-19) and Commentary on Building Code Requirements. Farmington Hills (MI): American Concrete Institute; 2019.
35. EC2. (2004). EN 1992-1-1:2004: Eurocode 2: Design of concrete structures—Part 1-1: General rules and rules for buildings". Incl. Corrigendum 1: EN 1992-1-1:2004/AC:2008, incl. Corrigendum 2: EN 1992-1-1:2004/AC:2010, incl. Amendment 1: EN 1992-1-1:2004/A1:2014.
36. Elstner, R. C. & Hognestad, E. Laboratory investigation of rigid frame failure. *J. Proc.* **53**(1), 637–668 (1957).
37. Mattock, A. H. Diagonal tension cracking in concrete beams with axial forces. *J. Struct. Div. ASCE* **95**(ST 9), 1887–1990 (1969).
38. Haddadin, M.J., Hong, S.T., Mattock, A.H. Stirrup effectiveness in reinforced concrete beams with axial force. *J. Struct. Div*. (1971).
39. Regan, P. E. Beams subjected to axial loads. *Imperial College Lond.* **1971**, 93–118 (1971).
40. Leonhardt, F., Rostasy, K., Macgregor, J. & Patzak, M. *Schubversuche an Balken und Platten bei gleichzeitigem Langszug, dAfStb Heft 275* (W. Ernst & Sohn, 1977).
41. Soresen, K., Loset, O. & Olsen, T. (1981). Investigation of the influence of axial tensile forces on the transverse shear strength. Report No. PP1-1-5, Det Norske Veritas, Oslo, Plus appendixes.
42. Bhide, S. B. & Collins, M. P. Influence of axial tension on the shear capacity of reinforced concrete members. *ACI Struct. J.* **86**(5), 570–581. https://doi.org/10.14359/3013 (1989).
43. Saul, R. & Koch, R. *Zur Schubtragfahigkeit von Stahlbetonplatten bei gleichzeitigem Langszug, Beton-und Stahlbetonbau 84, Heft 7* 181–186 (Ernst & Sohn Verlag, 1989).
44. Emrich, H. (1993). Zum Trgverhalten von Stahlbetonbauteilen unter Querkraft-unde Langszugbeansprunchung, Schriftenreihe des Instituts fur Massivbau und Bau stofftechnologie, Heft 20, Karlsruhe.
45. Adebar, P. & Collins, M. P. Shear strength of members without transverse reinforcement. *Can. J. Civ. Eng.* **23**(1), 30–41 (1996).
46. Tamura, T., Shigematsu, T., Hara, T. & Maruyama, K. A study of proposed design equation for the shear strength of R/C beams subjected to axial tension. *Doboku Gakkai Ronbunshu* **520**, 225–234 (1995).
47. Jorgensen, H. B., Hoang, L. C., Fabrin, L. S. & Malgaard, J. Influence of high axial tension on the shear strength of non-shear RC beams. *Poster Session Presented Proc. Int. IABSE Conf. Assess. Upgrading. Refurbishment. Infrastruct.* **99**(155), 161 (2013).
48. Fernández-Montes, D., González, V. E. & Díaz, H. E. Influence of axial tension on the shear strength of floor joists without transverse reinforcement. *Struct. Concr.* **16**(2), 207–220 (2015).
49. Limam, S., Nanaa, W. S. A., Bui, T. T., Limam, A. & Abouric, S. Experimental investigation and analytical calculations on shear strength of full-scale RC slabs with shear reinforcement for nuclear power plants. *Nucl. Eng. Des.* **324**(2017), 143–157 (2017).
50. MC. Fédération internationale du béton. fib Model Code for Concrete Structures 2010. Lausanne; 2013; 2010.
51. Deifalla, A. A strength and deformation model for prestressed lightweight concrete slabs under two-way shear. *Adv. Struct. Eng.* https://doi.org/10.1177/13694332211020408 (2021).
52. Deifalla, A. Torsional behavior of rectangular and flanged concrete beams with FRP. *J. Struct. Eng. ASCE.* https://doi.org/10.1061/(ASCE)ST.1943-541X.0001322 (2015).
53. Deifalla, A. F., Zapris, A. G. & Chalioris, C. E. Multivariable regression strength model for steel fiber-reinforced concrete beams under torsion. *Materials* **14**, 3889. https://doi.org/10.3390/ma14143889 (2021).
54. Deifalla, A. Refining the torsion design of fibered concrete beams reinforced with FRP using multi-variable non-linear regression analysis for experimental results. *Eng. Struct. Elsevier.* https://doi.org/10.1016/j.engstruct.2020.111394 (2021).

## Acknowledgements
First author acknowledges the support of Future University in Egypt and the second author acknowledges the support of King Fahd University of Petroleum & Minerals.

## Author contributions
A.D. wrote the main manuscript text and prepared figures. F.M.M. conducted analysis, reviewed the manuscript and prepared final script.

## Competing interests
The authors declare no competing interests.

## Additional information
**Correspondence** and requests for materials should be addressed to A.D.

**Reprints and permissions information** is available at www.nature.com/reprints.